

Tailoring electrocatalysts for *on-site* H₂O₂ production via two electron oxygen reduction

Jing Zhang[#], Danni Deng[#], Fangqiang Wang, Yu Bai, Yuchao Wang, Yingbi Chen, Peiyao Yang, Meng Wang, Houzheng Ou, Haitao Zheng, Yongpeng Lei^{*}

State Key Laboratory of Powder Metallurgy, Central South University, Changsha 410083, China

ABSTRACT: Hydrogen peroxide (H₂O₂) is a versatile green oxidant widely used in various fields. However, conventional synthesis methods such as the anthraquinone process suffer from high energy consumption, pollution, and safety risks. The electrocatalytic two-electron oxygen reduction reaction (2e⁻ ORR) offers a sustainable alternative by using O₂ and H₂O as feedstocks under ambient conditions, enabling *on-site* production with minimal environmental impact. This makes it a key research direction in the field. The main challenge for 2e⁻ ORR toward H₂O₂ lies in regulating the adsorption energy of the *OOH intermediate while preserving the O-O bond. Based on the reaction mechanism, this Review systematically summarizes recent progress in precious metal catalysts, carbon-based catalysts, metal oxide catalysts, and single-atom catalysts (SACs), along with on-site reactors and applications. It highlights current bottlenecks, including the trade-off among activity, selectivity, and stability, difficulties in large-scale synthesis, and limited real-world adaptability. Future efforts should focus on atomic-level catalyst design, green large-scale synthesis, system integration, and exploration of emerging catalytic systems. This Review aims to provide insights to accelerate the industrialization of electrocatalytic H₂O₂ production.

KEYWORDS: H₂O₂, Electrocatalysis, 2e⁻ ORR, Catalysts, *On-site* H₂O₂ reactors, Industrial application

1. Introduction

Hydrogen peroxide (H₂O₂) has undergone a century of industrial development,^[1-6] evolving from the early anthraquinone process laboratory trial in the 1930s to the mature large-scale production technology that currently dominates the global market, with the global annual output exceeding 5 million tons and a sustained annual demand growth rate of 5~8% driven by the green transformation of various industries.^[7-9] Diverse application fields exhibit distinct market demand

characteristics for H₂O₂: the chemical synthesis and pulp bleaching industries require high-concentration H₂O₂ (30~70 wt%) for continuous production,^[10-14] while water treatment, antibacterial disinfection, and green agriculture favor *on-site* produced low-to-medium concentration H₂O₂ (0.1~10 wt%) with low transportation and storage costs.^[15-19] In addition, the emerging fields such as electro-Fenton reaction for pollutant degradation and fuel cell power generation put forward higher requirements for the in-situ preparation capacity and purity of H₂O₂, which cannot be met by the

Received: March 24, 2026. **Revised** April 17, 2026. **Accepted:** April 10, 2026. **Available online:** May 8, 2026

Corresponding author: Yongpeng Lei – State Key Laboratory of Powder Metallurgy, Central South University, Changsha 410083, China; E-mail: lypkd@163.com; leiyongpeng@csu.edu.cn

Author Contributions: # Jing Zhang and Danni Deng contributed equally to this paper.

traditional centralized production mode.^[4,5,7]

And the current H₂O₂ synthesis technologies are facing prominent core bottlenecks in industrial scale-up, cost control and scenario adaptability, which seriously restrict the efficient utilization of H₂O₂ in various fields. Since the mid-20th century, the anthraquinone process has dominated industrial H₂O₂ production, accounting for over 95% of global output due to its ability to produce high-concentration H₂O₂ (30-70%).^[20-23] This process relies on the hydrogenation-oxidation cycle of 2-ethylanthraquinone and exhibits high technical maturity. However, amid the escalating emphasis on sustainable development, its inherent drawbacks have become increasingly prominent: (1) It requires high-temperature and high-pressure conditions, coupled with precious metal catalysts (e.g., Pd/Al₂O₃), leading to substantial equipment costs and energy consumption; (2) It depends on organic solvents (e.g., heavy aromatics), which pose risks of organic wastewater pollution; (3) The product necessitates complex extraction-distillation purification and cannot be prepared *on-site*, introducing explosion hazards during transportation.

Other alternative synthesis methods also suffer from limitations. The direct H₂O₂ synthesis method (via direct reaction of H₂ and O₂) avoids organic solvents but faces severe explosion risks in H₂/O₂ mixtures and low catalyst selectivity. The photocatalytic synthesis leverages solar energy but is constrained by rapid recombination of photogenerated carriers and low reaction efficiency, remaining confined to laboratory-scale research.^[24-26] In this context, the electrocatalytic 2e⁻ ORR has emerged as a research hotspot due to its green and safe nature.^[27, 28] **Figure 1** illustrates the number of publications and citations for this catalytic approach in the Web of Science database. This technology can realize the continuous decentralized production of H₂O₂ under mild conditions,^[29, 30] which not only reduces the cost and safety hazards of H₂O₂ storage and transportation, but also use renewable energy for *on-site* production on demand. Characterized by green, environmental friendliness, cost-effectiveness, and safety, it stands as a highly promising H₂O₂ synthesis approach.^[31, 32] The evolutionary timeline of H₂O₂ synthesis technologies is illustrated in **Figure 2**.^[33-38]

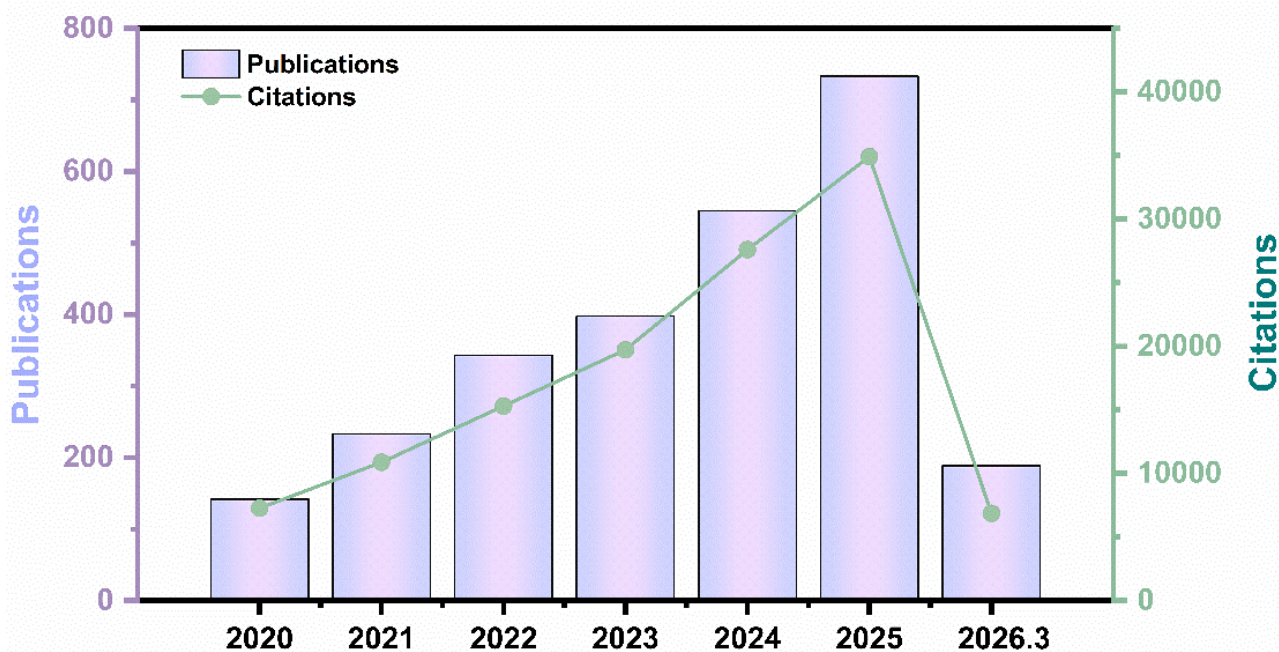


Figure 1. Annual publication and citation trends of research on electrocatalytic H₂O₂ production via two-electron oxygen reduction reaction over the recent 5 years. (Data source: Web of Science Core Collection. data for 2026 are as of March 2026)

Therefore, designing 2e⁻ ORR catalysts with high activity, high selectivity, and long stability remains a core challenge in this field. This review focuses on summarizing the latest advances in electrocatalytic 2e⁻

ORR for H₂O₂ production and applications (**Figure 3**). It emphasizes the current bottlenecks and innovative directions, which provides references for fundamental and industrial research.

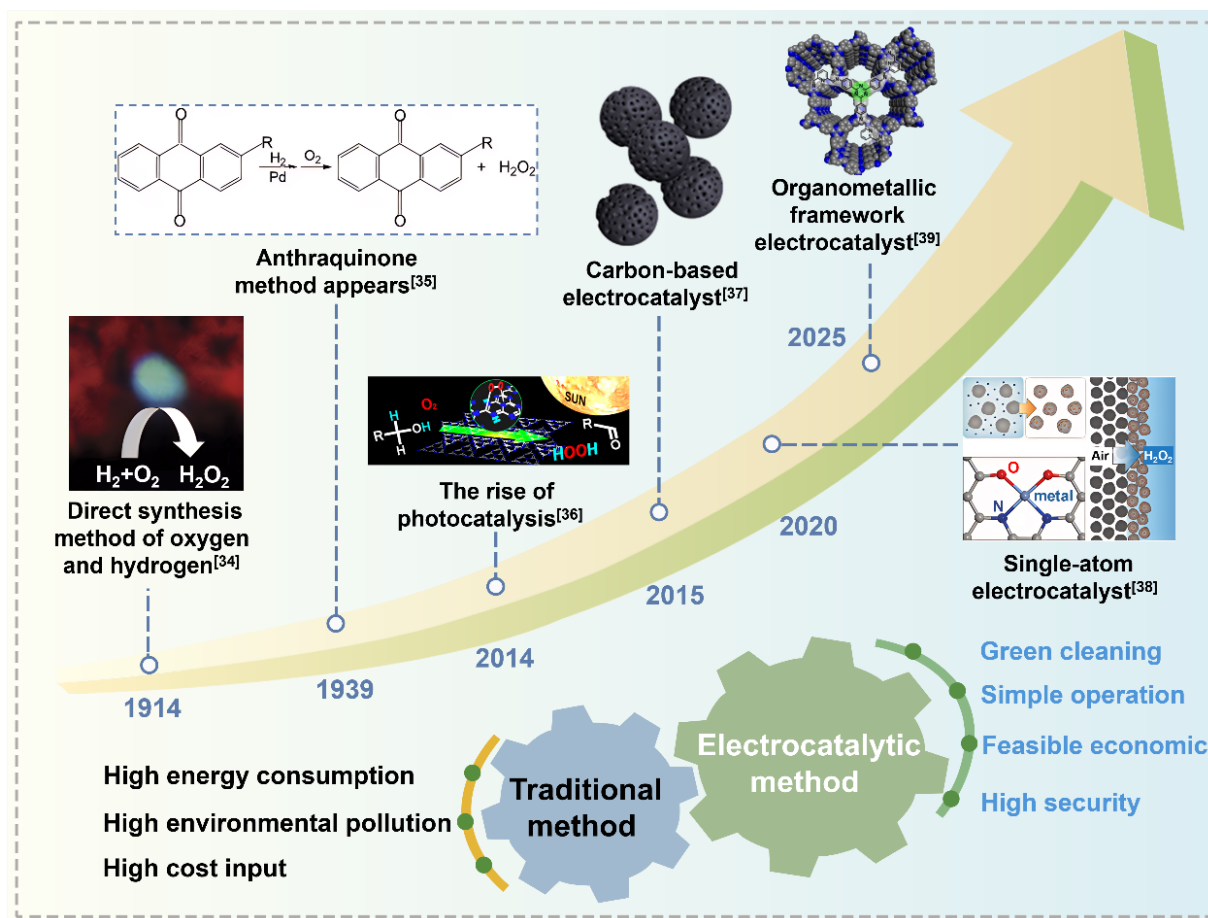
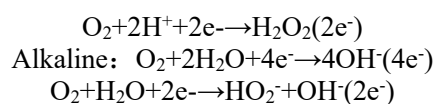
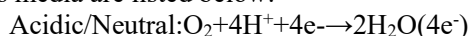


Figure 2. Innovation timeline of H₂O₂ preparation technology. Some inset figures are reproduced from ref.^[33] (Copyright 2008, Royal Society of Chemistry), ref.^[34] (Copyright 2021, Wiley-VCH), ref.^[35] (Copyright 2014, ACS Publications), ref.^[36] (Copyright 2015, Elsevier), ref.^[37] (Copyright 2020, Wiley-VCH), ref.^[38] (Copyright 2024, Wiley-VCH)

2. Reaction mechanism of electrocatalytic ORR for H₂O₂ production

2.1 Reaction mechanism

ORR involves multiple elementary steps, including O₂ adsorption, electron/proton transfer, and formation of oxygen-containing intermediates.^[39, 40] ORR is typically categorized into two pathways: the four-electron (4e⁻) pathway and the two-electron (2e⁻) pathway. Among them, the 4e⁻ pathway, which produces H₂O, serves as the core cathode reaction in metal-air batteries, whereas the 2e⁻ pathway is employed for the electrocatalytic synthesis of H₂O₂. The corresponding reaction equations of ORR in various media are listed below:^[41]



As shown in **Figure 4a**, the ORR process typically initiates with O₂ adsorption on the catalyst surface. Active sites bind O₂ in a specific configuration, while electrons transfer from the electrode surface to the active sites, thereby triggering subsequent processes such as bond cleavage, proton/electron transfer, and chemical reconstruction. Finally, the products desorb from the active sites and the electrode-electrolyte interface.^[43, 44] Specifically, O₂ adsorbed on the electrode surface first combines with a proton (H⁺) and an electron (e⁻) to form the *OOH intermediate. If the O-O bond of *OOH cleaves and further dissociates into *O and *OH, the ORR proceeds via the 4e⁻ pathway to produce H₂O. In contrast, if the O-O bond of *OOH remains intact and combines with an additional H⁺ and e⁻, the 2e⁻ pathway dominates, generating H₂O₂.^[45-47]

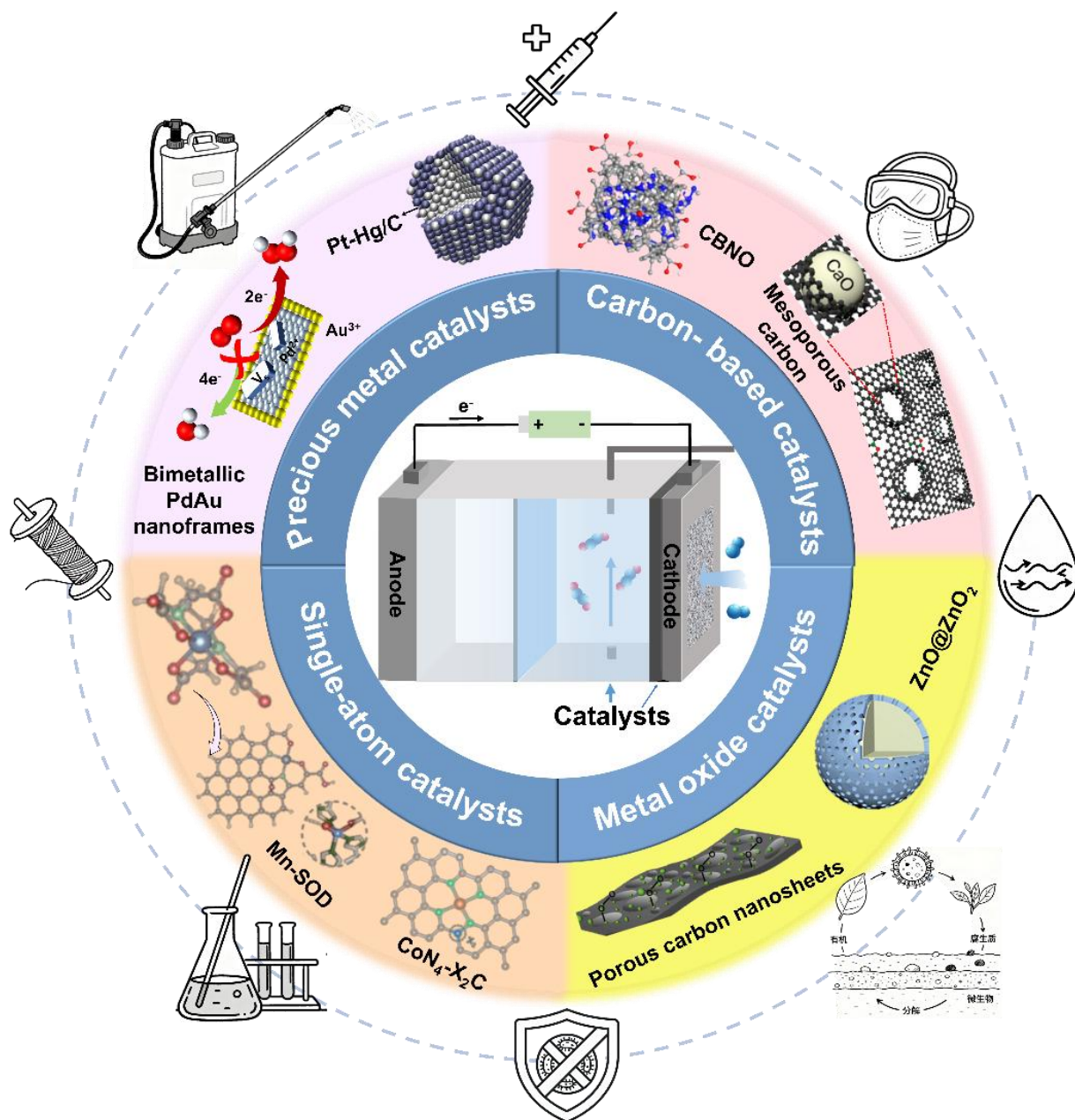


Figure 3. Core catalytic materials for electrocatalytic H_2O_2 production and H_2O_2 application fields. Some inset figures are reproduced from ref.^[31] (Copyright 2021, ACS Publications), ref.^[48] (Copyright 2020, Wiley-VCH), ref.^[78] (Copyright 2025, Wiley-VCH), ref.^[79] (Copyright 2024, Wiley-VCH), ref.^[86] (Copyright 2023, RSC Publishing), ref.^[87] (Copyright 2024, Springer Nature), ref.^[93] (Copyright 2023, Elsevier), ref.^[95] (Copyright 2024, Wiley-VCH)

Notably, the $4e^-$ ORR exhibits a more positive electrode potential and higher energy conversion efficiency, making it thermodynamically favored over the $2e^-$ pathway.^[48-50] Thus, suppressing the $4e^-$ pathway and promoting the $2e^-$ pathway is critical for efficient H_2O_2 synthesis. From the mechanism outlined above, the $2e^-$ ORR process hinges on the formation

and stabilization of the $^*\text{OOH}$ intermediate: cleavage of the O–O bond diverts the reaction to the $4e^-$ pathway, while retention of the O–O bond is a prerequisite for H_2O_2 generation^[51, 52]. Additionally, the binding strength between the $^*\text{OOH}$ intermediate and the catalyst surface plays a decisive role in determining the reaction pathway.^[53, 54]

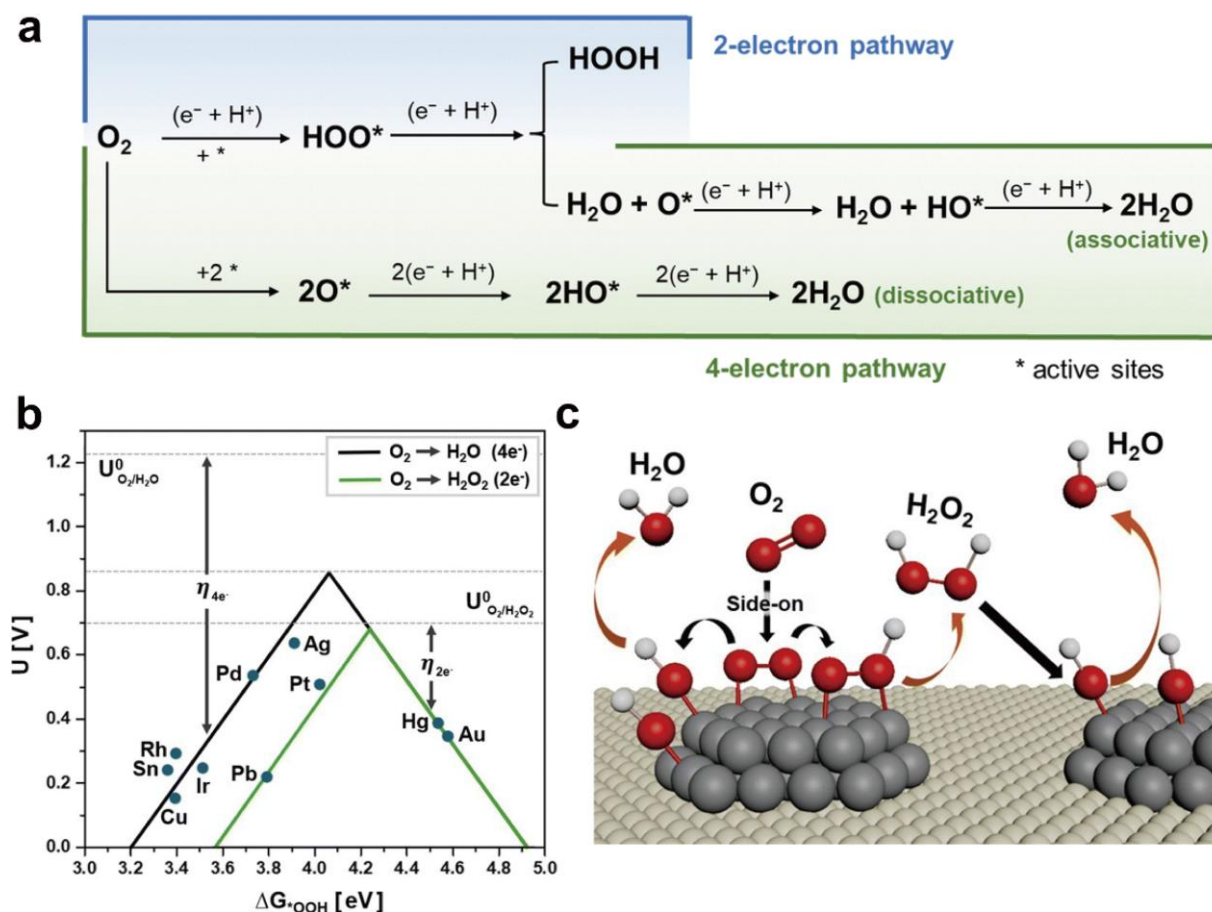


Figure 4. Reaction mechanism of electrocatalytic ORR for H₂O₂ production. (a) 4e⁻ and 2e⁻ reaction pathways, (b) Sabatier volcano plot of ORR on pure metal catalysts. (c) Schematic diagram of changes in the oxygen adsorption model of pure metals. Gray atoms represent active metals, and beige atoms represent carbon substrates.^[42] (Copyright 2024, Royal Society of Chemistry)

Figure 4b presents a Sabatier volcano plot illustrating the correlation between ORR potential and *OOH binding energy for different metals. Metals located on the left side of the volcano peak exhibit excessively strong *OOH adsorption, leading to prolonged residence of *OOH on the catalyst surface. This facilitates O-O bond dissociation into *OH and *O, favoring the 4e⁻ ORR pathway. Conversely, metals on the right side of the peak display weak *OOH adsorption, which slows the initial combination of O₂ molecules with H⁺, reducing the activity of 2e⁻ ORR for H₂O₂ synthesis.^[55, 56] These findings underscore that for the 2e⁻ ORR, both retention of the O-O bond and moderate *OOH adsorption energy are critical for efficient electrocatalytic H₂O₂ production. Therefore, controlling the catalyst's geometric structure and active site distribution is essential to facilitate end-on adsorption of *OOH (**Figure 4c**), inhibit O-O bond

cleavage, and promote the 2e⁻ pathway. This ultimately ensuring high H₂O₂ activity and selectivity.

2.2 Local reaction environment and reaction kinetics

In acidic media, the high proton (H⁺) concentration accelerates the proton-coupled electron transfer (PCET) process of the *OOH intermediate. Meanwhile, the high ionic strength compresses the electric double layer (EDL) near the catalyst surface, thereby enhancing the electrostatic interaction between the catalyst surface and the *OOH intermediate. Additionally, the ordered hydrogen bond network formed by interfacial water molecules improves proton transfer efficiency, but it may also compete with the *OOH intermediate for adsorption sites on the catalyst surface. In alkaline media, the high concentration of hydroxide ions (OH⁻) modulates the protonation degree of the *OOH

intermediate. The expanded EDL near the catalyst surface weakens the electrostatic interaction between the catalyst surface and the *OOH intermediate. Moreover, the disordered structure of interfacial water inhibits proton transfer, while effectively suppressing the non-selective decomposition of H₂O₂ (a common side reaction in acidic media).

The dynamic local pH near the catalyst surface, different from the bulk electrolyte pH, can regulate the reaction free energy barrier and further affects the catalytic performance by modulating the adsorption energy of the *OOH intermediate. For example, during the electrosynthesis of H₂O₂ in acidic media, an enhanced local alkaline microenvironment forms on the surface of F-doped carbon nanotubes (F-CNTs), significantly lowering the energy barrier for *OOH formation and improving oxygen transfer. Their synergistic effect boosts the selectivity toward H₂O₂ in acidic conditions.^[57]

3. Synthesis and characterization

Figure 5 summarizes the commonly used synthesis methods and characterization techniques for electrocatalytic H₂O₂ production. In catalyst preparation, the choice of synthetic approach is closely related to the specific demands of electrocatalytic H₂O₂ generation. Such catalysts are required to favor the 2e⁻ ORR pathway and enable precise regulation of active sites and electronic structures.^[58]

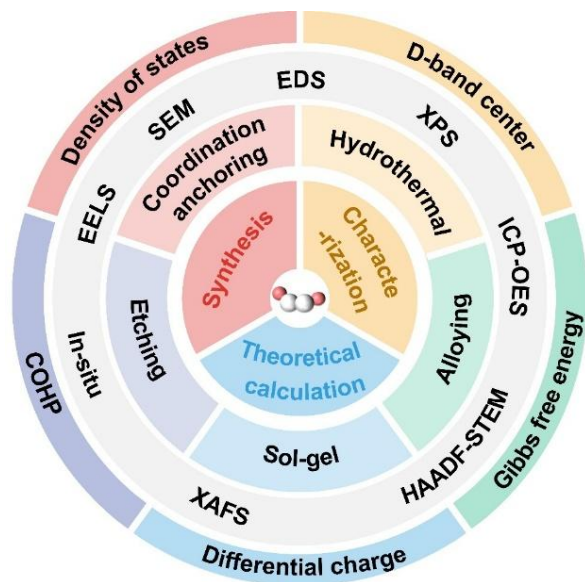


Figure 5. Main research methods for electrocatalytic 2e⁻ reduction to produce H₂O₂.

3.1 Synthesis methods

Catalysts for electrocatalytic H₂O₂ production can be prepared via various strategies, including the hydrothermal method, coordination anchoring method, alloying method^[8], etching method^[31], sol-gel method^[27], and defect engineering method. These methods are all centered around optimizing catalyst performance and achieve targeted regulation from dimensions such as morphology, active sites, and electronic structure.

Each approach exhibits distinct merits and inherent trade-offs. The hydrothermal method enables controllable crystal growth and uniform morphology under mild conditions, yet suffers from relatively low scalability, long reaction times, and limited batch-to-batch reproducibility. The coordination anchoring method achieves highly dispersed metal sites (especially for SAC) and strong metal-support interactions, but relies on elaborate ligand design and precise thermal control, which complicates large-scale preparation. Alloying method effectively modulates d-band centers and optimizes intermediate adsorption, improving both activity and selectivity. However, it often requires high-temperature treatment and precise elemental ratio control, potentially causing particle sintering and phase segregation. The etching method creates rich pores and surface defects to expose more active sites, but may cause structural collapse, excessive surface roughness, or reduced electrical conductivity. The sol-gel method provides homogeneous elemental mixing and tunable porosity at low temperatures, but involves slow gelation, high calcination temperatures, and possible shrinkage-induced structural damage. Finally, defect engineering method significantly enhances intrinsic activity by regulating charge distribution and intermediate binding, yet excessive defects can accelerate carbon corrosion, induce structural instability, and degrade long-term stability.

3.2 Characterization methods

At the characterization level, techniques such as Scanning Electron Microscopy (SEM) and High-Angle Annular Dark-Field Scanning Transmission Electron Microscopy (HAADF-STEM) are used to observe the microscopic morphology and dispersibility of the catalyst. X-ray Photoelectron Spectroscopy (XPS) and X-ray Absorption Fine Structure (XAFS) can analyze the chemical valence state and coordination environment of the active sites.^[59, 60]

Under practical ORR operating conditions, most $2e^-$ ORR catalysts undergo dynamic structural reconstruction, manifested as changes in the coordination environment and surface chemical state of active sites, and even the formation of new active phases, which directly determines catalytic performance. Studies have shown that the actual active sites are mostly reconstructed species rather than the pristine structure. The main reconstruction pathways include the evolution of single-atom catalysts from $M-N_x$ to $M-N_xO_y$, surface redox reactions and the formation of oxygen vacancies or oxide layers in metal oxides/chalcogenides, and surface segregation in noble-metal alloys; these processes significantly affect H_2O_2 selectivity by tuning the $*OOH$ adsorption energy.

Operando X-ray absorption spectroscopy (XAS) can accurately characterize the local coordination environment (coordination number, bond length) and valence state of metal active sites under operating conditions, and track the dynamic evolution of M-N/O bonds in single-atom catalysts and the oxidation state changes of precious metal active sites. In-situ attenuated total reflection surface-enhanced infrared absorption spectroscopy (ATR-SEIRAS) serves as a powerful tool to identify the degradation pathways of catalysts during long-term $2e^-$ ORR operation by dynamically tracking surface intermediates, functional groups, and structural evolution under realistic working conditions. It enables real-time detection of adsorbed $*OOH$, $*OH$, and H_2O_2 species, whose accumulation or abnormal transformation indicates excessive intermediate adsorption, non-selective decomposition, or the generation of reactive oxygen species (ROS) that induce carbon oxidation and active site damage. Additionally, in situ Raman spectroscopy is sensitive to the structural changes of carbon supports (e.g., carbon skeleton oxidation, defect generation) and the formation of oxygen-containing functional groups, and can also detect the dynamic changes of $*OOH$ intermediates and catalyst surface oxides during ORR. Furthermore, Mössbauer spectroscopy is especially suitable for the characterization of Fe-based catalysts, which can distinguish the different valence states and coordination environments of Fe active sites under operating conditions, and reveal the reconstruction of Fe-N-C single-atom catalysts.^[61,62]

The combination of multiple in situ/operando characterization techniques can realize the multi-dimensional and multi-scale characterization of catalyst reconstruction, which is of great significance for accurately identifying the real active sites of $2e^-$ ORR and revealing the intrinsic catalytic mechanism.

3.3 Theoretical calculation

In the context of theoretical calculations, the application of density functional theory (DFT) is particularly critical. By calculating key parameters including the d-band center, reaction energy barrier, density of states of active sites, differential charge density, and Crystal Orbital Hamilton Population (COHP), the favorable conditions for the $2e^-$ ORR pathway can be elucidated at the atomic scale. This not only provides guidance for the experimental optimization of catalyst structures but also ultimately enables the dual enhancement of efficiency and selectivity in electrocatalytic H_2O_2 production.^[63,64]

DFT calculations can predict the adsorption energy of key intermediates (e.g., $*OOH$), reaction free energy barriers, and the intrinsic activity of each candidate site. Correlating operando structural information with DFT-derived activity descriptors allows quantitative assignment of the catalytic contribution of each site, exclusion of non-active or spectator species, and clarification of whether the observed performance originates from the as-prepared structure or the dynamically reconstructed phase. This integrated strategy eliminates ambiguity in active-site identification and enables the establishment of a definitive, operationally relevant structure–activity relationship.^[65]

4. Yield calculation and performance evaluation criteria for H_2O_2 electrosynthesis

4.1 Yield calculation methods

Two core yield calculation methods are adopted to evaluate the catalytic efficiency of electrocatalysts for H_2O_2 production via the $2e^-$ ORR, with the concentration of H_2O_2 determined by classical titration methods or online electrochemical detection techniques:^[66,67]

4.1.1 H_2O_2 yield

It is usually expressed as the amount of H_2O_2 produced per unit mass of catalyst per unit time ($\text{mol g}_{\text{cat}}^{-1} \text{h}^{-1}$), the calculation formula is as follows:

$$Y = \frac{n(H_2O_2)}{t \cdot m_{\text{cat}}}$$

where n is the amount of generated H_2O_2 , t is the

electrolysis time, m_{cat} is the mass of the loaded catalyst. The concentration of H_2O_2 is determined via cerium sulfate titration^[67].

4.1.2 Faradaic efficiency (FE)

Defined as the ratio of the electric quantity consumed for H_2O_2 generation to the total electric quantity passed through the electrolysis system, it is a key indicator to reflect the electron utilization efficiency of the $2e^-$ ORR pathway, with the calculation formula:

$$\text{FE}(\%) = \frac{2CVF}{Q} \times 100\%$$

where V is the volume of electrolyte from the cathodic tank, F is the Faraday constant ($96,485 \text{ C mol}^{-1}$), C is the concentration of generated H_2O_2 from the cathodic tank, and Q is the passed charge during the electrolysis.

4.2 Core performance evaluation indicators

The core performance of electrocatalysts for H_2O_2 production via the $2e^-$ ORR is comprehensively evaluated by three key indicators, all of which are tested under standardized electrochemical conditions to ensure the comparability and reliability of catalytic performance data across different catalysts. The detailed definitions, testing methods and characterization criteria of each indicator are as follows:

4.2.1 Selectivity for H_2O_2

As the primary indicator for evaluating $2e^-$ ORR catalytic specificity, it refers to the percentage of oxygen molecules that are reduced to H_2O_2 via the $2e^-$ pathway relative to the total reduced oxygen molecules (excluding the $4e^-$ ORR pathway producing H_2O). It is quantitatively determined by the rotating ring-disk electrode (RRDE) technique, calculated from the measured disk current (total ORR current) and ring current (oxidation current of the generated H_2O_2 at the ring electrode). The standard test conditions are set as: electrode rotation speed of 1600 rpm, potential scanning range of 0.0 ~ 0.8 V (versus reversible hydrogen electrode, vs. RHE), and the selectivity value is expressed as a percentage (%). The calculation formula is as follows:

$$\text{H}_2\text{O}_2(\%) = 200 \times \frac{I_R / N}{I_R / N + I_D}$$

where I_D and I_R stand for disk current and ring current, respectively, and N is the calculated collection

efficiency. The calibration procedure for the N value is as follows: LSV curves are collected at different speeds in a N_2 saturated mixture of 0.1 M KOH + 10 mM $\text{K}_3[\text{Fe}(\text{CN})_6]$. During the test, $\text{Fe}(\text{CN})_6^{4-}$ was oxidized to $\text{Fe}(\text{CN})_6^{3-}$ by adding a constant potential of 1.2V versus RHE to the ring electrode potential. The corrected N value was 0.36.

4.2.2 Electrocatalytic activity

It reflects the reaction rate and kinetic performance of the catalyst for $2e^-$ ORR-driven H_2O_2 synthesis, and is characterized by two critical electrochemical parameters, both tested by linear sweep voltammetry (LSV) with a scan rate of 5 mV s^{-1} in an oxygen-saturated electrolyte:

Onset potential (E_{onset}): The initial potential where the $2e^-$ ORR reaction occurs, expressed in V (vs. RHE). A more positive onset potential indicates a lower reaction overpotential and better intrinsic catalytic activity of the catalyst.

H_2O_2 partial current density ($j_{\text{H}_2\text{O}_2}$): The current density dedicated exclusively to H_2O_2 generation at a specific applied potential, expressed in mA cm^{-2} . A higher partial current density means a faster $2e^-$ ORR reaction rate and higher H_2O_2 production efficiency per unit electrode area.

4.2.3 Catalytic stability

It is a key indicator for assessing the practical application potential of the catalyst, referring to the ability of the catalyst to maintain high H_2O_2 selectivity and electrocatalytic activity during long-term continuous electrolysis. It is evaluated by the chronoamperometry (CA) test under a constant applied potential (the potential corresponding to the maximum H_2O_2 selectivity of the catalyst). The stability is characterized by two parameters: current retention rate (the ratio of the final current to the initial current after electrolysis) and H_2O_2 selectivity attenuation rate (the percentage of selectivity reduction after electrolysis). An excellent catalyst shows a current retention rate of over 80% and a negligible selectivity attenuation ($\leq 5\%$) after long-term testing, without obvious active site loss or catalyst structure degradation.

5. Electrocatalysts for the synthesis of H_2O_2 via $2e^-$ ORR

Electrocatalysts serve as the foundation for $2e^-$ ORR-mediated H_2O_2 synthesis. An ideal $2e^-$ ORR

catalyst should exhibit characteristics such as high ORR activity, excellent electrical conductivity, fast mass transfer rate, and low economic cost.^[68, 69] Additionally, it needs to possess high 2e⁻ ORR selectivity and catalytic stability to ensure continuous, efficient H₂O₂ production, thereby ensuring that the

catalyst can produce H₂O₂ efficiently and stably. Currently, typical 2e⁻ ORR catalysts mainly encompass precious metal catalysts, carbon-based catalysts, metal oxide catalysts, and SACs.^[70, 71] A performance comparison of different catalysts in recent years is summarized in **Table 1**.

Table 1. Performance comparison of various catalysts in recent years.

Samples	Onset potential (V vs. RHE)	H ₂ O ₂ selectivity (%)	H ₂ O ₂ Yield (mol g _{cat} ⁻¹ h ⁻¹)	Stability (h)	References
ppy-ZnN ₃	~0.78	92	43	48 (-0.38 V vs RHE)	<i>Angew. Chem. Int. Ed.</i> 2025 , 64, e202421864.
TPDA-BDA COF	0.72	89.7	-	50 (2 mA cm ⁻²)	<i>Angew. Chem. Int. Ed.</i> 2025 , 64, e202424720.
Se ₂ -Pt	-	95	4.16	400 (250 mA cm ⁻²)	<i>Nat. Commun.</i> 2024 , 15, 9346.
Pb SA/OSC	~0.76	94	-	100 (50 mA cm ⁻²)	<i>Nat. Commun.</i> 2024 , 15, 193.
FeN ₃ O ₂	0.77	95	29.6	10 (200 mA cm ⁻²)	<i>Nat. Commun.</i> 2024 , 15, 10758.
Pd/MCS-8	0.70	95	15.77	12 (0.3 V vs RHE)	<i>Angew. Chem. Int. Ed.</i> 2024 , 63, e202403023.
O _v -Bi ₂ O ₃ -EO	~0.65	90	-	12 (0.4 V vs RHE)	<i>Adv. Mater.</i> 2024 , 36, 2408341.
CoNCB	0.76	~100	4.72	5 (20 mA cm ⁻²)	<i>Nat. Commun.</i> 2024 , 15, 4079.
P-NMG-10	0.78	91	30	24 (~40 mA cm ⁻²)	<i>Nat. Commun.</i> 2023 , 14, 4430.
FS-CFs	0.814	99.1	-	-	<i>Adv. Mater.</i> 2023 , 36, 2208533.
CBNO	0.67	95	2.89	24 (100 mA cm ⁻²)	<i>Angew. Chem. Int. Ed.</i> 2024 , 63, e202317267.
ZnO@ZnO ₂	0.46	~100	5.47	40 (0.3 V vs RHE)	<i>Energy Environ. Sci.</i> 2023 , 16, 3526
.NiO _x -C	0.69	90.7	-	-	<i>ACS Catal.</i> 2022 , 12, 5911.

5.1. Precious metal catalysts

Certain precious metal materials exhibit good catalytic activity and H₂O₂ selectivity in the 2e⁻ ORR process, making them among the most extensively studied catalytic materials at present. In recent years, there have been many research reports on exploring the 2e⁻ ORR performance of precious metals such as platinum (Pt), palladium (Pd), and gold (Au). Typically, various strategies are employed, including regulating the surface structure of materials and introducing a second metal for alloying, to improve their yield.

To address key challenges in the 2e⁻ ORR for H₂O₂ electrosynthesis, Siahrostami et al.^[8] designed a PtHg₄ electrocatalyst for the 2e⁻ ORR. The *OOH binding energy of PtHg₄ was near the volcano peak, with an overpotential lower than 0.1 V, and its H₂O₂ selectivity reached 95% in the potential range of 0.35~0.55 V, outperforming Au/C catalysts in both activity and selectivity. To achieve tunability in the adsorption of oxygen-containing species on the catalyst surface, Jing and colleagues^[50] immobilized palladium nanoparticles (Pd NPs) on a carbon substrate with customizable surface properties, preparing Pd/MCS-8 by supporting Pd NPs on mesoporous carbon spheres. The

mesoporous structure of the carbon support facilitated O₂ enrichment and increased local pH, constructing a favorable reaction microenvironment for the 2e⁻ ORR. The interaction between Pd NPs and the carbon support optimizes the adsorption energy of the reaction intermediate *OOH at the edges of carbon active sites, thereby enabling efficient H₂O₂ electrosynthesis (**Figure 6a** and **b**).

As for the need for optimizing *OOH adsorption energy, enhancing H₂O₂ selectivity, and accelerating reaction kinetics in the 2e⁻ ORR, Yu's research team^[51] prepared Se₂-Pt nanoparticles by constructing a Pt-Se shell on the surface of Pt crystal nuclei. The amorphous Pt-Se shell exhibits a moderate O₂ adsorption capacity, which can form stress to improve the *OOH adsorption energy, enhance H₂O₂ selectivity, and accelerate reaction kinetics. After optimizing the shell thickness, the selectivity of electrocatalytic synthesis of H₂O₂ reached 95% (Fig. 6c and d). Meanwhile, outperforming pure Au catalysts, Zhao and co-workers^[31] prepared bimetallic PdAu nanoframes (PdAu-nf) through a series of processes, including CO reduction, low-temperature displacement, and acid etching, and studied their 2e⁻ ORR performance. PdAu-nf has more stable adsorption for *OOH, with H₂O₂ selectivity greater than 90% in the potential range of

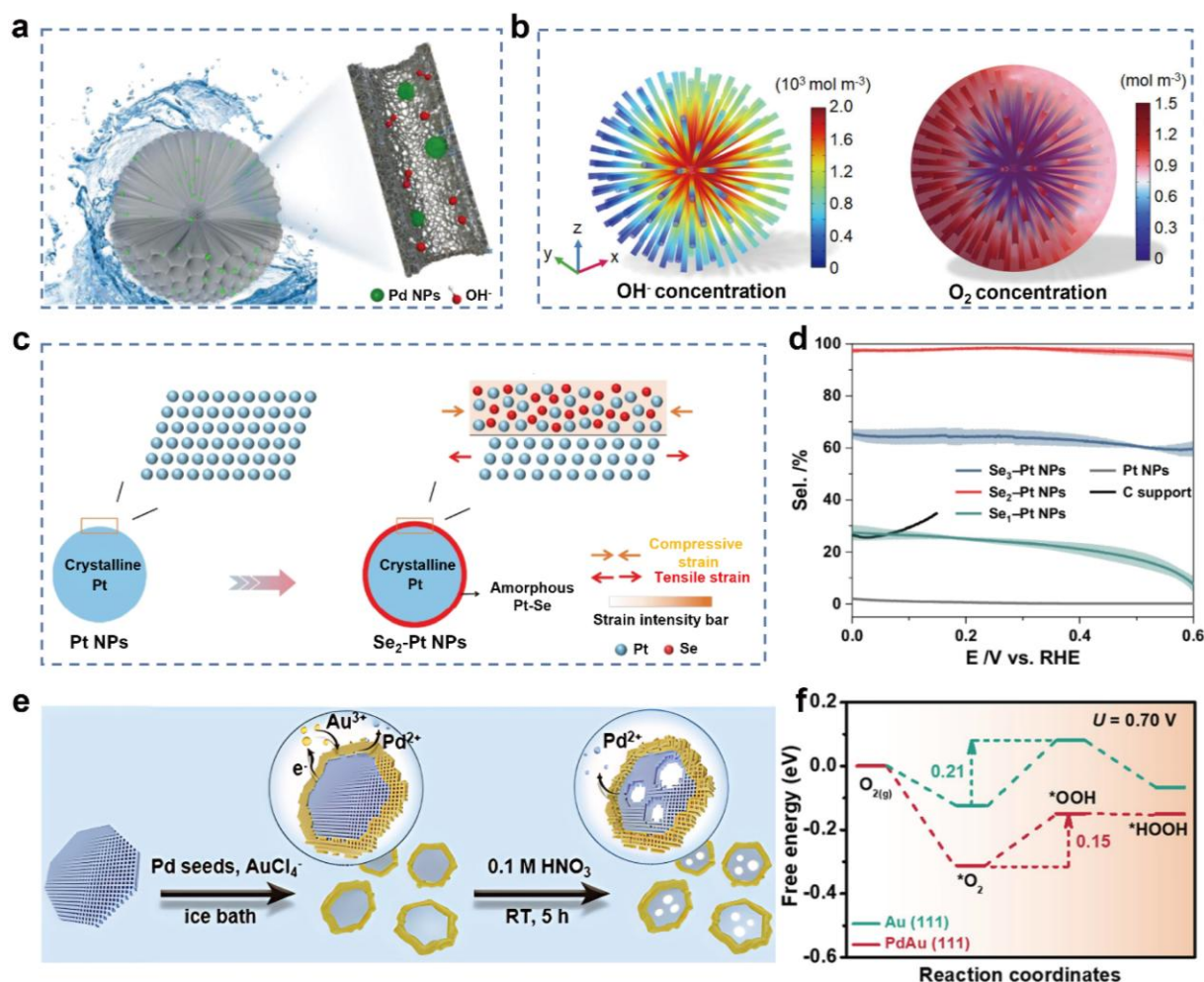


Figure 6. Research on some precious metal materials. (a) Schematic diagram showing the advantages of Pd/MCS-8 in efficient 2e⁻ ORR. (b) Spatial distribution of OH⁻ and O₂ concentration.^[50] (Copyright 2024, Wiley-VCH) (c) Schematic diagram of the synthesis process of Se₂-Pt nanoparticles and the corresponding structural evolution of the surface. (d) Selectivity values (%) calculated from rotating ring-disk electrode (RRDE) polarization curves.^[51] (Copyright 2024, Springer Nature) (e) Schematic diagram of the preparation of palladium-gold nanoframes through stepwise growth and etching in solution. (f) Free energy changes during the 2e⁻ ORR to generate H₂O₂ on Au(111) and PdAu(111) surfaces at a potential of 0.7 V.^[31] (Copyright 2021, American Chemical Society)

0~0.5 V, which is better than that of pure Au catalysts (Figure 6e and f).

The scarcity and high cost of precious metals remain key barriers to their large-scale application. The crustal abundance of noble metals such as Pt and P is only on the order of 10⁻⁹ to 10⁻⁸, and the cost of purification and preparation is high, making it difficult to meet the demand for catalyst dosage in industrial-scale H₂O₂ production. In addition, some precious metal catalysts (such as pure Pt) are prone to dissolution or agglomeration during long-term electrolysis, leading to the loss of active sites, which further limits their practical application scenarios. To address this, researchers are turning to non-noble metal catalysts.

5.2 Carbon-based catalysts

Carbon materials offer low cost, abundant reserves, tunable morphology, high surface area, and good conductivity.^[73] However, they face challenges such as low ORR activity and low H₂O₂ selectivity. In recent years, aiming to optimize the electrocatalytic H₂O₂ production process with carbon-based materials as catalysts, research efforts have primarily focused on developing regulatory strategies including structural engineering, defect engineering, heteroatom doping, surface functionalization, or the synergistic coupling of multiple strategies to enhance the catalytic activity and H₂O₂ selectivity of carbon-based catalysts.^[74-75]

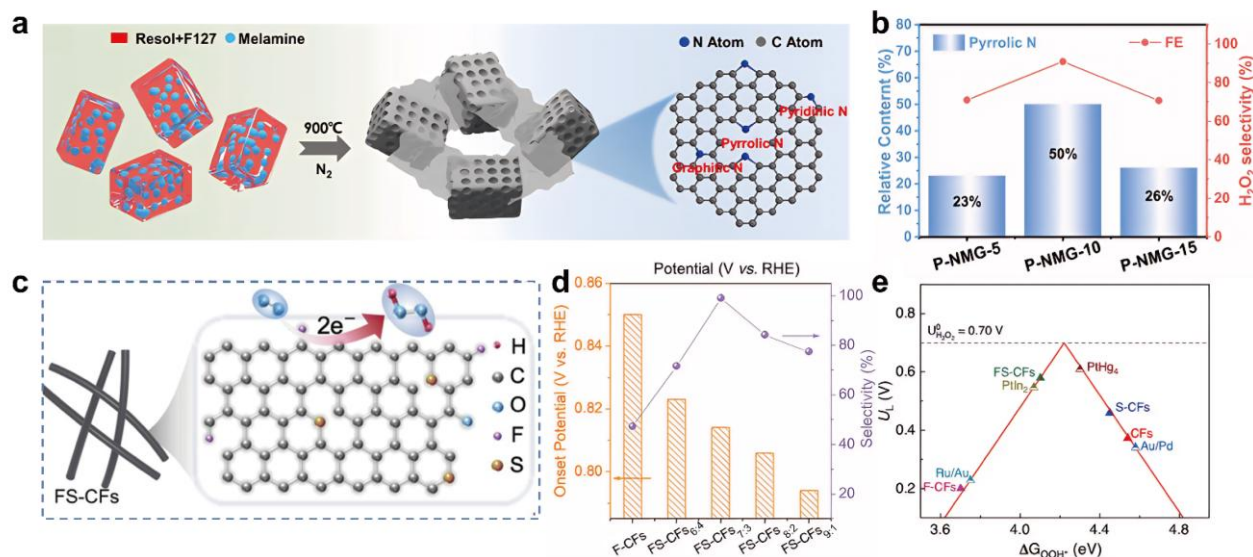


Figure 7. Research on some carbon-based catalytic materials. (a) Schematic diagram of the synthesis of P-NMG-X series materials, (b) Relationship between pyrrole N content and H₂O₂ selectivity.^[76] (Copyright 2023, Springer Nature) (c) Schematic diagram of FS-CFs structure, (d) Onset potentials and selectivities of FS-CFs and comparative samples. (e) Theoretical electrocatalytic activity volcano plot for varied F/S doping configurations.^[77] (Copyright 2023, Wiley-VCH)

To tackle the need for providing more ORR reaction environments for pyrrole nitrogen and reducing the reaction energy barrier of the 2e⁻ ORR, Peng et al.^[76] designed a pyrrole-nitrogen-rich doped graphene mesoporous carbon composite (P-NMG-10) by constructing pore structures and defect sites. The defects provide more ORR reaction environments for pyrrole nitrogen, reduce the energy barrier of the 2e⁻ ORR reaction, and the selectivity for H₂O₂ reaches 90% (Figure 7a and b). Researchers led by Xiang^[77] prepared fluorine (F) and sulfur (S) co-doped metal-free carbon fiber catalysts (FS-CFs) via electrospinning and pyrolysis. The co-doping of F and S enhances charge transfer and electron spin redistribution, and the adjacent F and S atoms also change the electronic structure of carbon active sites, thereby enhancing the adsorption of *OOH on the active sites and improving the reaction activity and selectivity. FS-CFs exhibited a high onset potential of 0.814 V, with H₂O₂ selectivity exceeding 85% in the potential range of 0.5–0.8 V, and the yield and FE were 29.3 mol g_{cat.}⁻¹ h⁻¹ and 98.01%, respectively, outperforming most reported carbon-based or metal-based electrocatalysts (Figure 7c–e).

Due to the issues of strong *OOH interaction with planar B₄C sites, insufficient O₂ accumulation, and unwanted HER side reactions in 2e⁻ ORR, Choi and colleagues^[78] developed a mesoporous B-doped carbon catalyst (meso-BPC) featuring curved B₄C sites by adding a pore-forming agent. In contrast to the planar

B₄C structure, the curved B₄C sites formed in the porous carbon exhibit a weaker interaction with *OOH. Moreover, its porous structure facilitates the accumulation of more O₂ and mitigates the HER side reaction. The H₂O₂ selectivity of B₄C reached 88%, with a yield and FE of 119.32 mg h⁻¹ cm⁻² and 88%, respectively (Figure 8a and b). To overcome challenges related to the difficult generation and stabilization of *OOH intermediates, Song's group^[79] developed a novel carboxylated h-BN/G heterojunction (CBNO) by adopting a strategy combining boron (B) and nitrogen (N) co-doping with surface carboxyl functionalization. The carboxylated h-BN/G configuration effectively retains a large number of O–O bonds, which is beneficial to the generation and stabilization of *OOH intermediates. At the same time, it can lower the reaction energy barriers of the *OOH → *HOOH and *HOOH → H₂O₂ processes, thereby improving the 2e⁻ ORR catalytic performance and promoting the generation of H₂O₂ (Figure 8c and d).

Currently, carbon-based catalysts still exhibit some limitations: some metal-free doped carbon materials are improved through complex hierarchical pore structure design; at the same time, under strong alkaline or long-term electrolysis conditions, the oxygen-containing functional groups on the surface of the carbon skeleton are prone to desorption, resulting in the loss of active sites.

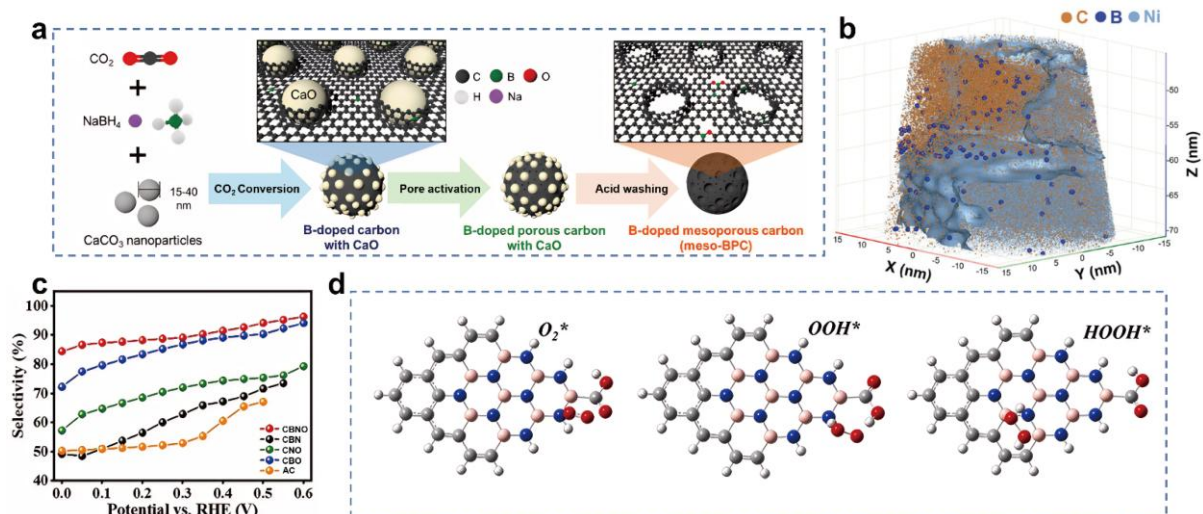


Figure 8. Research on some carbon-based catalytic materials. (a) Schematic diagram of the synthesis process and atomic structure of mesoporous boron phosphide carbon (meso-BPC). (b) Three-dimensional atomic map reconstructed by atomic probe tomography (APT) measurement.^[78] (Copyright 2025, Wiley-VCH) (c) H_2O_2 selectivity of different samples. (d) Adsorption configurations of different oxygen species in CBNO.^[79] (Copyright 2023, Wiley-VCH)

5.3 Metal oxide catalysts

Metal oxide are gaining attention for their abundance, low cost, stability, and tunable coordination.^[80-82] Meanwhile, their unique electronic structures and adjustable coordination environments are also conducive to systematically studying their reaction mechanisms and structure-activity relationships.^[83, 84] Currently, the active sites of metal oxide are mainly adjusted and optimized through design strategies such as morphology, crystal texture structure, and micro-topological structure, thereby improving their activity and selectivity in the $2e^-$ ORR.^[85]

Focusing on the issues of unwanted $4e^-$ ORR inhibition of pure In_2O_3 , Wu et al.^[27] developed a variety of $\text{In}_2\text{O}_3/\text{CDs}$ -based catalysts that employed carbon dots (CDs) as cocatalysts. The primary active sites are concentrated on In_2O_3 , while CDs can modulate the interfacial electron transfer kinetics and slow down the process. This ensures that insufficient electrons are delivered to O_2 molecules, inhibiting the $4e^-$ ORR. Among them, $\text{In}_2\text{O}_3/\text{CDs}$ -10 achieved nearly 100% H_2O_2 selectivity, which was much higher than 72% of In_2O_3 , and its H_2O_2 yield was $4.5 \text{ mol g}_{\text{cat}}^{-1} \text{ h}^{-1}$, which was better than that reported in the literature. As for challenges including limited active sites for $2e^-$ ORR and excessively strong binding energies of *OOH and *O intermediates, Zhou's team^[86] designed a $\text{ZnO}@\text{ZnO}_2$ electrocatalyst. Where the *in-situ* growth of octahedral ZnO_2 on tetrahedral ZnO

forms a heterointerface, providing active sites for $2e^-$ ORR. It also weakens the binding energy of *OOH and *O intermediates, thereby promoting excellent $2e^-$ ORR activity with a selectivity of 97.75~100%. At 0.1 V, the yield and FE were $5.47 \text{ mol g}_{\text{cat}}^{-1} \text{ h}^{-1}$ and 95.5%, respectively (Figure 9a and b).

In Wu's work,^[87] by regulating the crystallinity of the metal oxide and the pore structure of the carbon support, it was found that amorphous NiO_x and moderate Ni-OH bond strength can make the *OOH intermediate tend to be adsorbed on amorphous $\text{NiO}_x\text{-C}$ through the end-on mode, while the mesoporous structure of the carbon nanosheets can promote O_2 adsorption and improve the H_2O_2 selectivity (maximum 91% within 0.15~0.60 V), with performance superior to crystalline materials (Figure 9c and d).

However, metal oxide still suffer from inherent limitations of insufficient conductivity and poor uniformity of active sites: the electronic conductivity of most metal oxides is only $10^{-4}\sim 10^{-2} \text{ S} \cdot \text{cm}^{-1}$, and they need to be compounded with carbon materials to meet the requirements of electron transport; at the same time, traditional preparation processes easily lead to agglomeration of active sites or uneven distribution of vacancies, affecting the precise regulation of *OOH adsorption energy.

5.4 Single-atom catalysts

SACs feature atomically dispersed active sites,

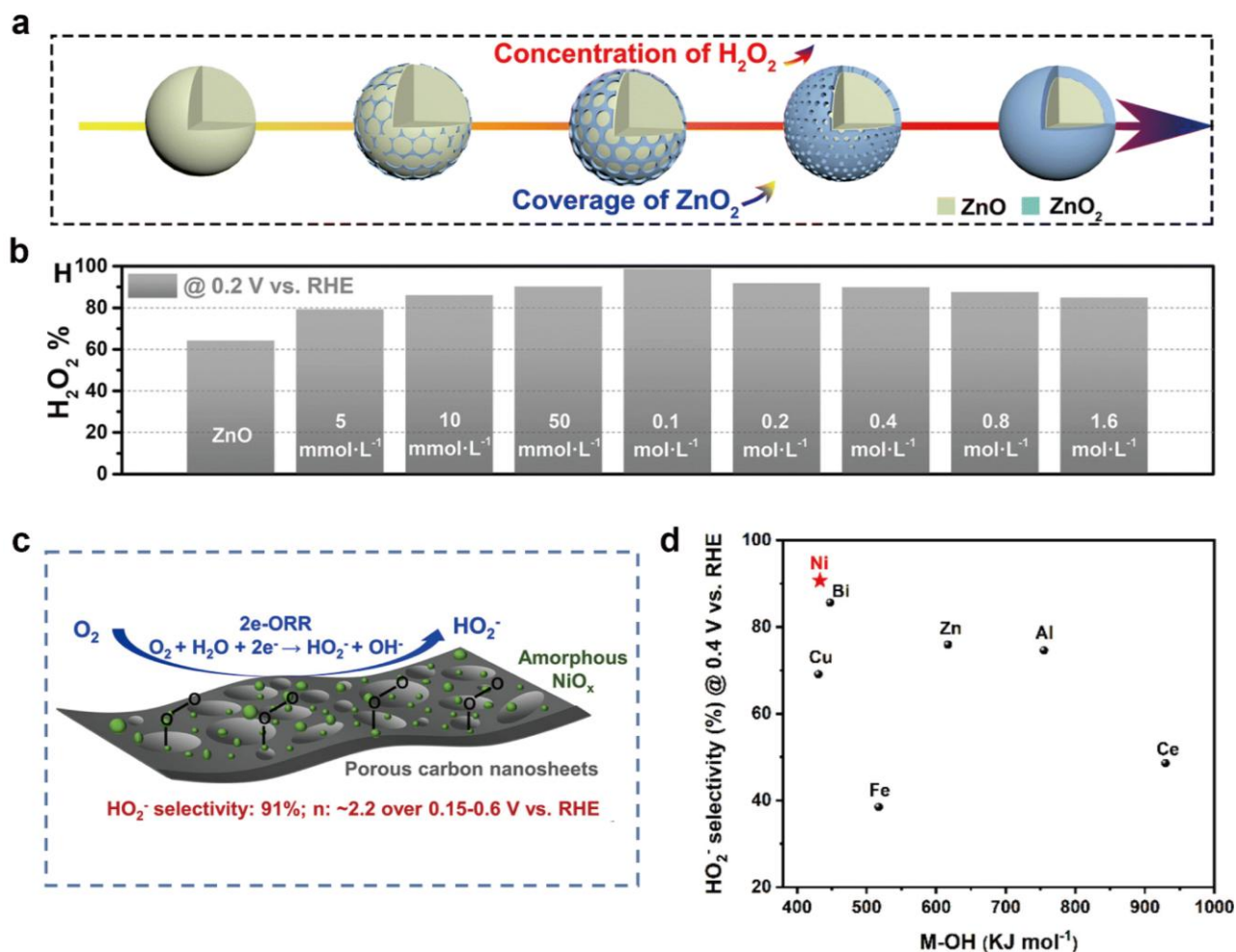


Figure 9. Research on some metal oxide catalytic materials. (a) Schematic diagram of the coverage of ZnO₂ on ZnO as a function of H₂O₂ concentration. (b) H₂O₂ selectivity of ZnO treated with different concentrations of H₂O₂.^[86] (Copyright 2023, RSC Publishing) (c) Schematic diagram of NiO_x catalytic process. (d) Relationship between M-OH bond strength and H₂O₂ selectivity.^[87] (Copyright 2022, American Chemical Society)

offering high metal utilization and uniform active centers. Moreover, the electronic structure and coordination environment of the metal centers are highly tunable, which is more conducive to the top adsorption of O₂ molecules and tends to the 2e⁻ ORR path. They are a type of promising catalytic material for the electrochemical synthesis of H₂O₂.^[88-91]

To reduce chemical/electrochemical decomposition during H₂O₂ electrochemical synthesis, Du's research team^[91] prepared a carbon black-supported Co-N-C SACs (CB@Co-N-C) and weakened the chemical/electrochemical decomposition by adjusting the catalytic layer thickness, thereby improving the 2e⁻ ORR selectivity. In addition to selecting appropriate central metal atoms, the coordination environment also

plays a crucial role in determining reaction selectivity. Chen et al.^[92] designed a series of Zn-N₄ SACs with pyrrole/pyridine nitrogen (N_{Po}/N_{Pd}) synergistic coordination through temperature control. They found that reasonable adjustment of the coordination of N_{Po}/N_{Pd} in the Zn-N₄ configuration can achieve a *OOH adsorption strength close to the optimal value, achieving a performance superior to that of configurations with a single N species. Among them, the H₂O₂ selectivity of ZnNC-700 can reach up to 97%, and the maximum yield and FE reached 11.2 mol g_{cat}⁻¹ h⁻¹ and 90% respectively (Figure 10a-c). Additionally, to regulate the eccentricity distance of Co atoms and enhance the adsorption energy of *OOH intermediates, Liu and colleagues^[93] reported an

atomically dispersed asymmetric cobalt catalyst (CoNCB). Compared with the square symmetric Co-N₄ configuration, the asymmetric Co-C/N/O configuration regulates the eccentricity distance of Co atoms and

enhances the adsorption energy of *OOH intermediates. The selectivity reached 95% in the potential range of 0.45~0.75 V, with the yield and FE being 4.72 mol g_{cat.}⁻¹ h⁻¹ and 60% respectively (Figure 10d).

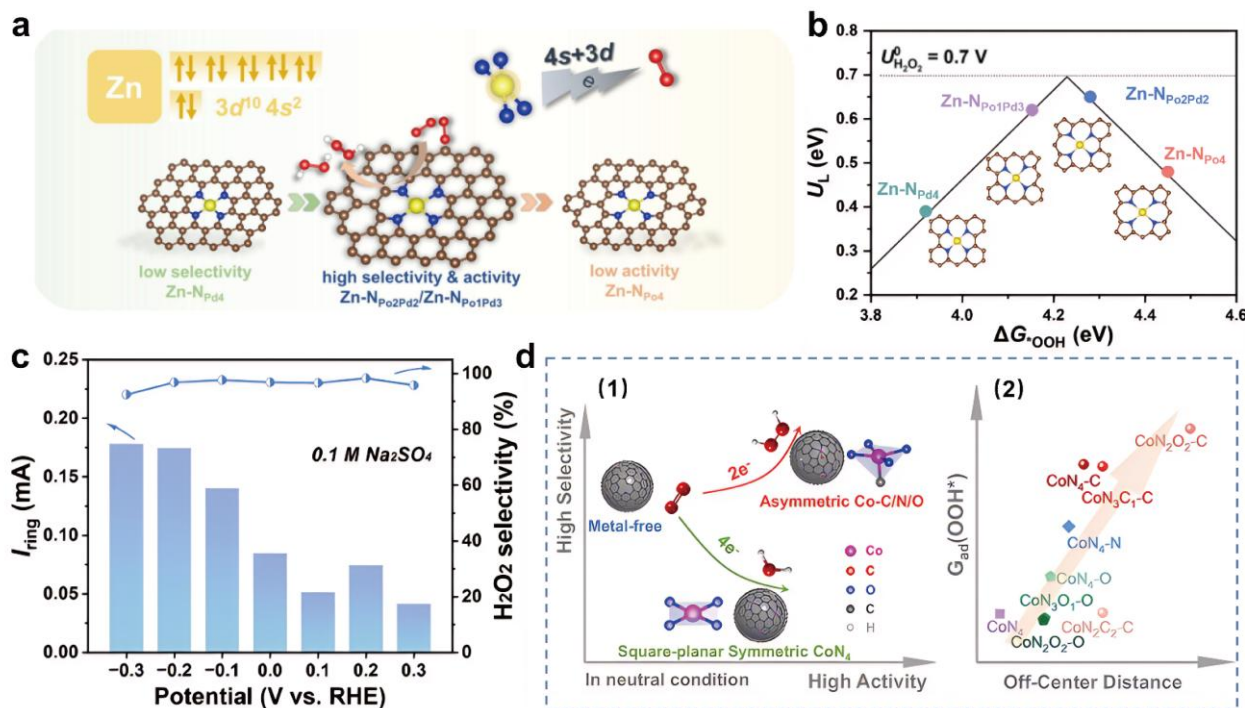


Figure 10. Research on some single-atom catalytic materials. (a) Schematic diagram of the mechanism of Zn-N₄ SACs with different N_{Po}/N_{Pd} coordination environments. (b) Calculated catalytic activity volcano plot for H₂O₂ production via 2e⁻ORR pathway. (c) Ring current obtained by linear sweep voltammetry (LSV) on a rotating ring-disk electrode (RRDE) in oxygen-saturated 0.1 M sodium sulfate solution, and the corresponding H₂O₂ selectivity of ZnNC-700.^[92] (Copyright 2024, Elsevier) (d) Schematic diagram of EHPP selectivity and activity of centrally symmetric CoN₄ and asymmetric Co-C/N/O electrocatalysts in 0.1 M PBS (pH=7) (1); relationship between the eccentricity distance of Co atoms and the adsorption energy of *OOH (2).^[93] (Copyright 2024, Springer Nature)

Focusing on a typical Co-N-C SACs, Chen and researchers^[94] investigated a typical Co-N-C SACs catalyst and obtained CoN₄-B₃C by introducing B atoms into the second coordination layer. B is doped at the B₃ position of the second coordination layer, which modifies the catalytic atomic interface, enhances the proton affinity on the catalyst surface, promotes the combination of *O at the front end of *OOH with protons, and this favors the 2e⁻ ORR pathway (Figure 11a and b). Inspired by natural enzymes containing Mn, Zeng's group^[95] prepared an N, O co-coordinated Mn SACs catalyst (Mn CD/C) on a carbon dot carrier. The maximum H₂O₂ selectivity of Mn CD/C reached 95.8%, with the yield and FE being 8.68 mol g_{cat.}⁻¹ h⁻¹ and 80% respectively (Figure 11c-e).

However, challenges remain for the large-scale synthesis and long-term stability of SACs. On the one

hand, single-atom metals (such as Mn, Co) tend to migrate and aggregate during high-temperature preparation or long-term electrolysis, leading to the loss of active sites. On the other hand, the metal loading of most SACs is low (usually < 5 wt%), which is insufficient to meet the demand for a high active site density required for industrial-scale H₂O₂ production. Moreover, the synthesis is challenging and it is difficult to precisely fabricate the ideal catalyst.

6. Deactivation mechanisms and stability enhancement strategies

6.1 Deactivation mechanisms

Catalytic stability is one of core indicators for

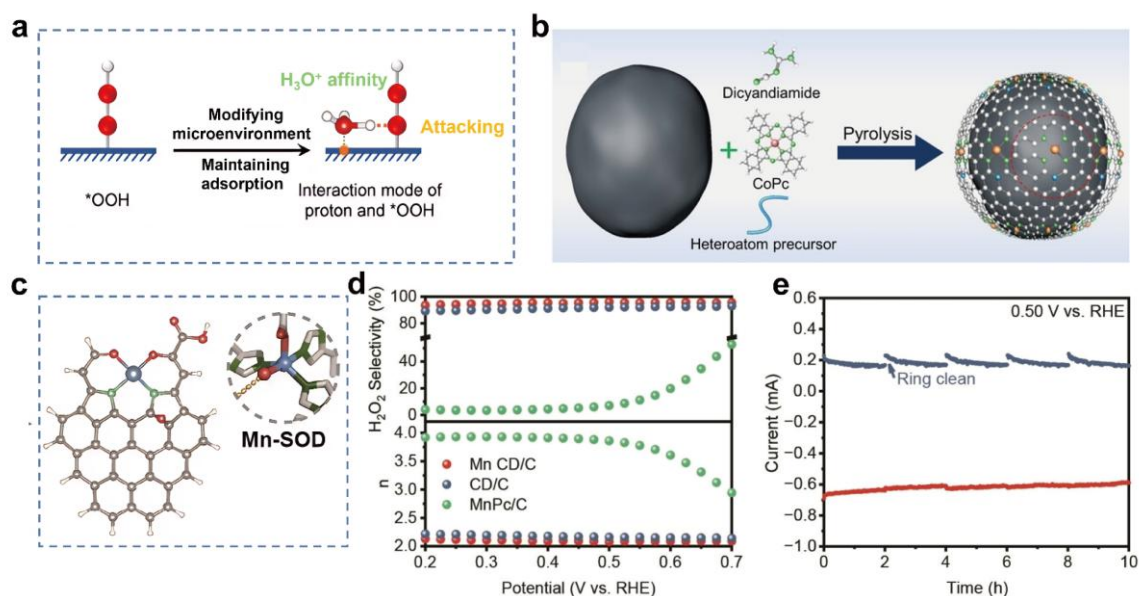


Figure 11. Research on some single-atom catalytic materials. (a) Research strategy of Co₁-NBC (b) Schematic diagram of the typical preparation process of heteroatom-doped cobalt SACs.^[94] (Copyright 2024, Wiley-VCH) (c) Schematic diagram of Mn CD synthesis. (d) Chronoamperometry test of Mn CD/C at 0.50 V. (e) H₂O₂ selectivity and electron transfer number.^[95] (Copyright 2024, Wiley-VCH)

evaluating the practical application potential of 2^{e-} ORR catalysts, which is closely related to the service life and industrialization feasibility of electrocatalytic H₂O₂ production systems. Under long-term ORR operating conditions (acidic/alkaline electrolytes, continuous applied potential, and so on), 2^{e-} ORR catalysts are prone to various degradation pathways, mainly including carbon corrosion, metal leaching, active sites reconstruction and agglomeration and H₂O₂-induced oxidative degradation.

6.1.1 Carbon corrosion

Carbon-based supports (e.g., porous carbon, graphene, carbon nanotubes) are widely used in 2^{e-} ORR catalysts due to their high conductivity and large specific surface area. However, in the ORR process, the hydroxyl radicals ($\cdot\text{OH}$) generated by the spontaneous decomposition of H₂O₂ can oxidize the carbon skeleton, leading to the destruction of the carbon support structure, the loss of active site anchoring sites, and the reduction of catalyst conductivity.^[96] Carbon corrosion is more severe in acidic electrolytes and at high applied potentials, which is a major degradation pathway for carbon-based and single-atom catalysts with carbon supports.

6.1.2 Metal leaching

In acidic or alkaline electrolytes, metal catalysts (e.g., Pd, Ni, Sn, etc.) may undergo oxidation reactions

due to changes in electrode potential, causing metal ions to dissolve from the catalyst surface into the electrolyte. In addition, the coordination structure on the catalyst surface may change during the reaction, weakening the metal-support interaction and making metal atoms more prone to detachment. And under industrial-level current densities, the reaction rate accelerates, and electron transfer and ion diffusion on the metal surface intensify, increasing the risk of metal leaching. Metal leaching directly causes the loss of active sites, resulting in a sharp decline in catalytic activity and selectivity.^[97]

6.1.3 Active sites reconstruction and agglomeration

During electrocatalysis, the active sites of metal single-atom catalysts (e.g., Ni, Co, etc.) may undergo irreversible reconstruction with potential variation, such as transformation from atomically dispersed states into metal nanoclusters, resulting in the reduction or loss of active sites and degraded catalytic activity. Moreover, under long-term operation, metal atoms can migrate and agglomerate driven by thermal motion and electrochemical effects, which further deteriorates the overall catalytic performance.^[97]

6.1.4 H₂O₂-induced oxidative degradation

The in-situ generated H₂O₂ and its decomposition products ($\cdot\text{OH}$, O₂⁻) have strong oxidative properties, which can oxidize the surface of metal active sites or

modify the electronic structure of catalytic interfaces. For example, the amorphous Pt-Se shell in Se²⁻-Pt nanoparticles can be oxidized by H₂O₂ to form PtO_x and SeO₄²⁻, leading to the destruction of the shell structure and the loss of the regulated *OOH adsorption energy. In addition, the oxygen vacancies in metal oxide catalysts can be occupied by oxygen atoms from H₂O₂ decomposition, resulting in the reduction of O₂ activation capacity.^[51]

6.2 Stability enhancement strategies

To mitigate the above degradation pathways and improve the long-term catalytic stability of 2e⁻ ORR catalysts, targeted and actionable strategies are proposed based on recent research advances.

6.2.1 Engineering catalyst design

Strengthen the interaction between metal active sites and supports by optimizing the coordination environment (e.g., introducing second coordination sphere heteroatoms, constructing bimetallic active sites) to inhibit metal leaching. Moreover, construct a protective shell (e.g., inert metal oxides, carbon layers, metal-organic frameworks (MOFs)) on the surface of catalyst active sites to isolate the direct contact between active sites and electrolytes/H₂O₂. The core-shell structure can effectively address critical issues including low selectivity and poor stability encountered in electrocatalytic H₂O₂ production by regulating the electronic structure and surface properties of catalysts.^[98,99]

Modify the surface of carbon supports with inert materials (e.g., polytetrafluoroethylene (PTFE), boron nitride (BN)) to form a hydrophobic and anti-oxidative coating, which reduces the adsorption of ·OH on the carbon surface and inhibits carbon corrosion. In addition, introducing heteroatoms (e.g., B, F, P) to form cross-linking bonds with the carbon skeleton can enhance the structural stability of the carbon support and prevent the desorption of oxygen-containing functional groups.^[100] Meanwhile, hydrophobic/hydrophilic functionalization of the catalyst surface and the construction of a hydrophobic-hydrophilic gradient structure facilitate oxygen transfer and proton conduction, thereby inhibiting parasitic reactions.^[101]

6.2.2 Regulating reaction environment

Reaction environment can be regulated via pH adjustment and electrolyte optimization. Tuning the electrolyte pH creates a local alkaline or acidic microenvironment to suppress side reactions such as the hydrogen evolution reaction and hydrogen peroxide

decomposition, thereby enhancing reaction selectivity and stability.^[57] Meanwhile, selecting suitable electrolyte components and concentrations (e.g., buffer-containing electrolytes) stabilizes the pH and ionic strength of the reaction system, mitigating electrolyte-induced corrosion or interference toward the catalyst.

6.2.3 System integration and protection

System integration can be achieved through membrane electrode assembly (MEA) and radical scavenging. MEA technology integrates the catalyst layer, electrolyte membrane, and gas diffusion layer to optimize interfacial contact and mass transport, thereby enhancing the overall stability.^[101] Meanwhile, radical scavengers can be introduced into the reaction system, or the intrinsic radical-scavenging capability of the catalyst can be utilized to suppress side reactions such as Fenton-like reactions, protecting both the catalyst and the product.

These strategies are often employed in combination, and synergistic optimization is achieved through multiscale engineering (atomic, micro, and macro levels) to realize the efficient and stable operation of electrocatalytic hydrogen peroxide production.

7. On-site H₂O₂ reactors

7.1 Research progress in on-site H₂O₂ reactors

Based on the core requirements for the electrochemical synthesis of H₂O₂ via 2e⁻ ORR, reactor design has evolved around three key objectives: enhancing selectivity, improving mass transfer efficiency, and adapting to industrial-scale applications. It leads to the development of mainstream technical pathways such as flow cells, membrane electrode assembly (MEA) reactors, proton exchange membrane (PEM) reactors, solid-state electrolyte (SSE) reactors, and coupled reactors.

Flow cell reactors enhance mass transfer via electrolyte circulation, making them suitable for medium to high concentration H₂O₂ production. The reactor is primarily composed of a gas diffusion electrode (GDE) loaded with the catalysts, an electrolyte circulation channel, an oxygen inlet pipeline, a current collector and a sealed reaction chamber. The GDE serves as the cathode to realize direct contact between O₂ and the catalytic active sites, eliminating the mass transfer limitation caused by the low solubility of O₂ in aqueous electrolytes; the electrolyte circulation channel accelerates the renewal

of the reaction interface and the desorption of H_2O_2 products, while the current collector ensures efficient electron transfer during the electrocatalytic reaction. Inspired by nature, Zeng et al.^[95] designed N_2O -

coordinated Mn sites (Mn CD/C) and assembled a flow cell (**Figure 12a**). In this configuration, O_2 directly contacts Mn CD/C, circumventing the issue of low O_2 solubility in aqueous electrolytes.

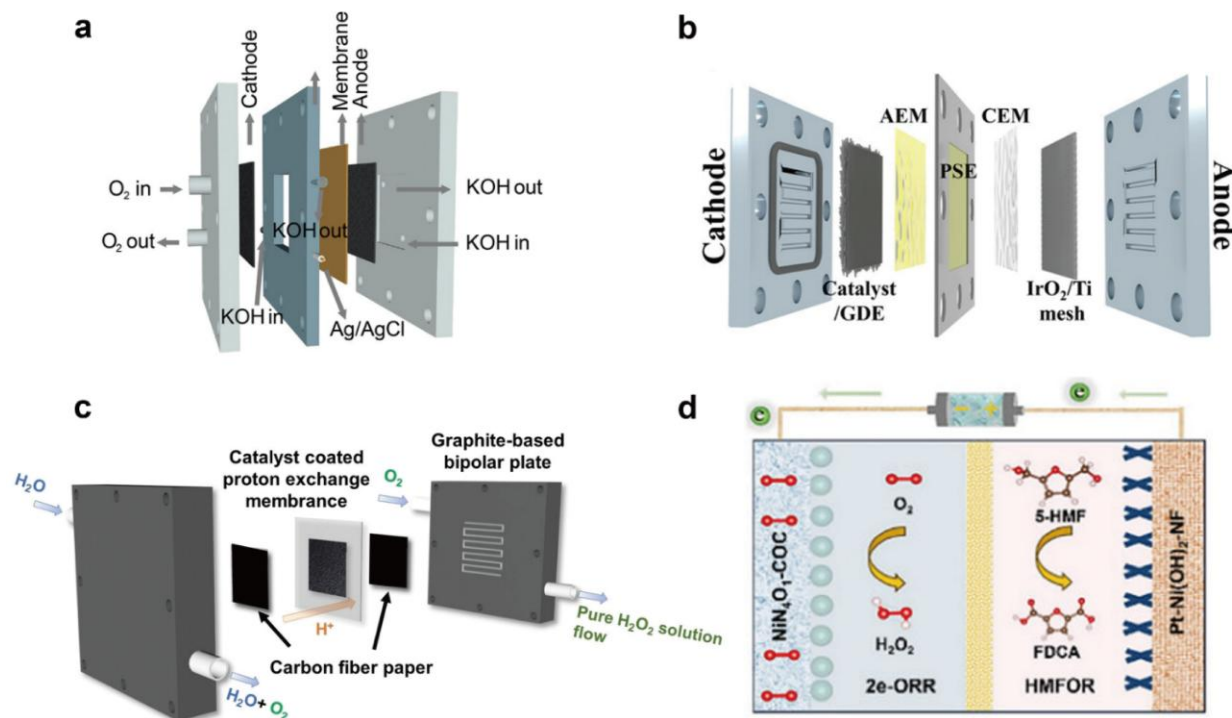


Figure 12. Research on some on site H_2O_2 reactor. (a) Scheme of the flow cell.^[95] (Copyright 2024, Wiley-VCH) (b) Schematic of the assembly of each part of the internal structure.^[98] (Copyright 2025, Wiley-VCH) (c) Schematic diagram of the graphite-based PEM electrolyzer for the continuous production of high-concentration H_2O_2 liquid flow.^[102] (Copyright 2024, Wiley-VCH) (d) Schematic diagram of the coupled $2e^-$ ORR || HMFOR system.^[103] (Copyright 2025, Wiley-VCH)

MEA reactors, utilizing flow field design and gas diffusion electrodes, overcome mass transfer limitations and enable high-concentration H_2O_2 synthesis at high current densities. Nevertheless, catalyst detachment reduces reactivity and stability, and H_2O_2 decomposition at the membrane interface also lowers the overall yield. SSE reactors incorporate a porous solid-state electrolyte interlayer at the membrane interface to prevent direct contact between the liquid electrolyte and the catalyst, thereby avoiding electrode flooding. By introducing pure water or a carrier gas into the interlayer, adjustable concentrations of high-purity H_2O_2 solution can be obtained without post-reaction separation or purification, making it suitable for various decentralized applications. Miao and co-workers^[98] proposed a strategy involving cation vacancy generation via self-optimizing reconstruction of metal-organic frameworks, achieving efficient H_2O_2 electrosynthesis at industrial-grade current densities in solid-state electrolyte reactors (**Figure 12b**). Its core

components include a catalyst layer with cation vacancies, a porous solid-state electrolyte interlayer (PSE), an anion exchange membrane (AEM), a cation exchange membrane (CEM), an IrO_2/Ti mesh anode and a double-chamber reaction module. The PSE interlayer is the key functional component, which isolates the liquid electrolyte from the cathode catalyst layer to avoid electrode flooding and active site deactivation; the AEM and CEM achieve selective ion transport, and the IrO_2/Ti mesh acts as a high-stability anode for the oxygen evolution reaction (OER) to match the cathodic $2e^-$ ORR.

PEM reactors, valued for their high proton conductivity and ease of product separation, are a key research focus for acidic $2e^-$ ORR, with recent advances centered on catalyst-membrane-electrode interface optimization. Chen and colleagues^[102] designed a series of cobalt porphyrin-based molecular catalysts supported on reduced graphene oxide ($\text{CoTPP}@RGO$). A PEM electrolyzer using this catalyst at the cathode (with pure

water at the anode) continuously produced ~7 wt% pure H₂O₂ solution for over 200 hours at a low cell voltage of ~2.1 V and a current density of 400 mA cm⁻² (Figure 12c). This reactor features a graphite-based bipolar plate, a high-conductivity PEM as the core separator, a CoTPP@RGO modified cathode catalyst layer, a pure water anode chamber, a liquid flow channel and a gas-tight sealing assembly. The graphite bipolar plate undertakes dual functions of current conduction and reaction interface support, and the PEM enables rapid proton transport from the anode to the cathode while preventing the mixing of cathodic and anodic products. The liquid flow channel is designed to realize continuous production and collection of high-concentration H₂O₂ solution.

Coupled reactors, which integrate the 2e⁻ ORR with other reactions, represent an emerging direction. By replacing the OER with an alternative anodic oxidation reaction, overall energy efficiency is improved. In Nie's work, [103] a novel Ni-N-C SAC featuring Ni-N₄O₁ coordination was designed. This SAC successfully realized the coupling of cathodic 2e⁻ ORR and anodic oxidation of 5-hydroxymethylfurfural (5-HMF). At a current density of 50 mA cm⁻², the overpotential for 5-HMF oxidation was only 0.32 V, which is considerably lower than that of the conventional OER process (Figure 12d). The integrated reactor consists of a Ni-N₄O₁ SAC modified cathode, a 5-hydroxymethylfurfural (5-HMF) oxidation anode, a carbon fiber paper current carrier, a proton exchange membrane and a co-electrolysis reaction cell. The cathode is dedicated to the 2e⁻ ORR for H₂O₂ generation, and the anode replaces the traditional OER with the selective oxidation of 5-HMF to 2,5-furandicarboxylic acid (FDCA); the proton exchange membrane realizes proton balance between the two electrodes, and the carbon fiber paper ensures efficient mass and electron transfer at the electrode-electrolyte interface.

7.2 Design of *on-site* H₂O₂ reactors

By rationally tuning porosity, hydrophobicity, and thickness according to reactor type, the three-phase interface can be stabilized, product desorption accelerated, and degradation pathways (such as carbon corrosion and active-site leaching) mitigated, thereby bridging catalyst design and reactor engineering toward practical high-performance H₂O₂ electrosynthesis.

In flow cells employing GDEs, the catalyst layer must be designed with hierarchical porosity to enable rapid gas-phase O₂ diffusion from the backing layer to active sites, while moderate hydrophobicity (typically

90–120° water contact angle) is introduced to prevent electrode flooding and suppress H₂O₂ accumulation and decomposition. The catalyst layer thickness is usually controlled within 5–20 μm to balance sufficient active-site loading and minimal mass-transport resistance.[104] In contrast, for submerged three-electrode cells, which rely on dissolved O₂, the catalyst should possess higher overall porosity and enhanced hydrophilicity to ensure full electrolyte wetting and efficient diffusion of dissolved oxygen; excessive hydrophobicity is avoided because it severely limits O₂ availability. The catalyst layer is generally thinner (3–10 μm) to minimize the diffusion distance of dissolved O₂ and avoid local O₂ depletion.[105]

8. *On-site* H₂O₂ applications

H₂O₂ is an inorganic chemical with strong oxidizing and weak reducing characteristics. At room temperature, it is a colorless, transparent liquid that dissolves easily in water. Its main feature is that the decomposition products are solely water and oxygen, with no secondary pollutants. With the advancement of environmental protection concepts and technological iteration, H₂O₂, relying on this advantage, has been applied in various fields such as antibacterial disinfection, water treatment, organic matter degradation, and green agricultural production, becoming a key chemical with both practicality and sustainability.[14, 67]

8.1 Antibacterial

H₂O₂ has powerful oxidizing properties. When it comes into contact with bacteria, it rapidly decomposes to produce nascent oxygen (O₂) and hydroxyl radicals (·OH). These reactive oxygen species can damage the cell walls and cell membranes of bacteria, as well as internal biological macromolecules such as proteins and nucleic acids, thereby disrupting bacterial metabolism and reproduction and exerting a bactericidal effect. Compared with strategies using antibiotics and metal ions (such as Ag, Cu), H₂O₂ offers a stronger, broad-spectrum antibacterial effect and a reduced risk of inducing bacterial resistance.

To achieve the continuous production of high-concentration pure H₂O₂ and full-spectrum antibacterial activity, Zhang et al.[106] designed a nickel phthalocyanine-based COF electrocatalyst (BBL-PcNi). By integrating it into a large electrolytic cell, it can continuously produce a relatively pure H₂O₂ solution with a concentration of up to 3.5 wt%.

Moreover, it exhibited strong antibacterial activity under full-spectrum irradiation (**Figure 13a**). Addressing the dual-stage needs of “rapid antibacterial action” and “long-term healing promotion” in infected wound treatment, Huang’s research team^[107] developed a CPO-Alg hydrogel (based on calcium peroxide and alginate). Through the dual spatial niche design of CPO NPs (calcium peroxide nanoparticles) within the gel framework, it achieved the biphasic release of H₂O₂: when used for infected wounds, the weakly constrained CPO NPs release rapidly, and the high concentration of H₂O₂ can eliminate bacteria and biofilms to exert the

initial antibacterial effect, and subsequently can continuously promote the proliferation of healing cells (**Figure 13b-d**). For synergistically enhancing antibacterial, anti-biofilm, and anti-inflammatory effects, Wu and colleagues^[108] synthesized Zn⁰@ZIF-8 through a simple stirring-physical grinding method, which can in situ generate a large amount of H₂O₂ through the 2e⁻ ORR. The galvanic corrosion of Zn⁰ in Zn⁰@ZIF-8 promotes simultaneous *in-situ* production of H₂O₂ and release of Zn²⁺, thereby enhancing antibacterial, anti-biofilm, and anti-inflammatory effects synergistically.

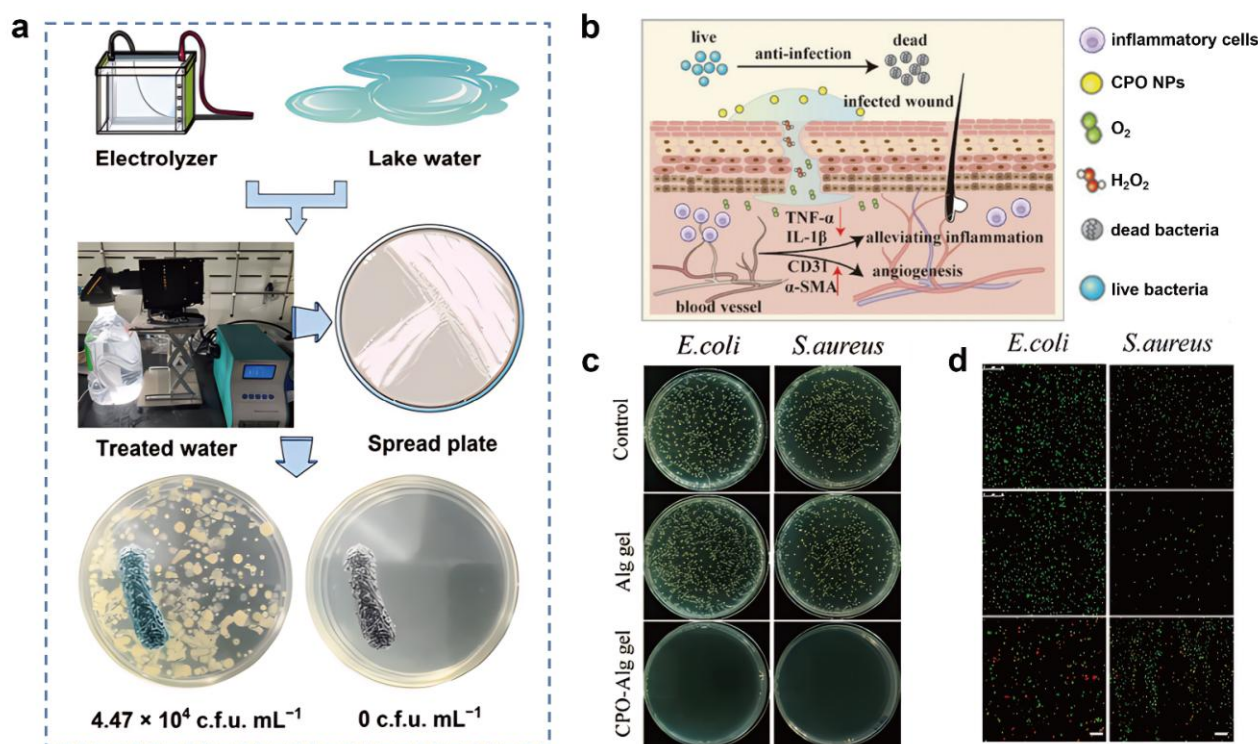


Figure 13. Partial studies on H₂O₂ disinfection and sterilization. (a) Schematic illustration of the antibacterial properties of the generated solution under full-spectrum irradiation.^[106] (Copyright 2024, American Chemical Society) (b) Schematic diagram of their application for infected wound healing. (c) Photographs of bacterial colonies of *S. aureus* and *E. coli* on agar plates after different treatments. (d) Fluorescence images of live/dead bacterial staining in different treatment groups. Scale bar: 15 μ m.^[107] (Copyright 2024, Wiley-VCH)

8.2 Water treatment

Driven by the need for water pollution control and the assurance of water quality safety, H₂O₂ has emerged as a key functional reagent in the field of water treatment due to its strong oxidizing properties and no secondary pollution characteristics.

To efficiently achieve electrocatalytic activation of H₂O₂ and enhance \cdot OH generation for strong bactericidal performance, Wen and co-workers^[109] developed a chainmail catalyst consisting of nitrogen-

doped carbon (NC)-encapsulated Co₃O₄ (NC@Co₃O₄). Co₃O₄ withdraws electrons from NC, which strengthens the affinity between oxygen atoms in H₂O₂ and electron-deficient carbon sites in NC and promotes the cleavage of the O–O bond. As a result, the \cdot OH generation rate catalyzed by NC@Co₃O₄ was 6.5 times higher than that of NC alone. When employed as the cathode in a flow-through electrochemical reactor, this system enabled over 6.8-order-of-magnitude (99.99998%) inactivation of *Escherichia coli* in tap water at an applied voltage of only 2 V (**Figure 14a and b**).

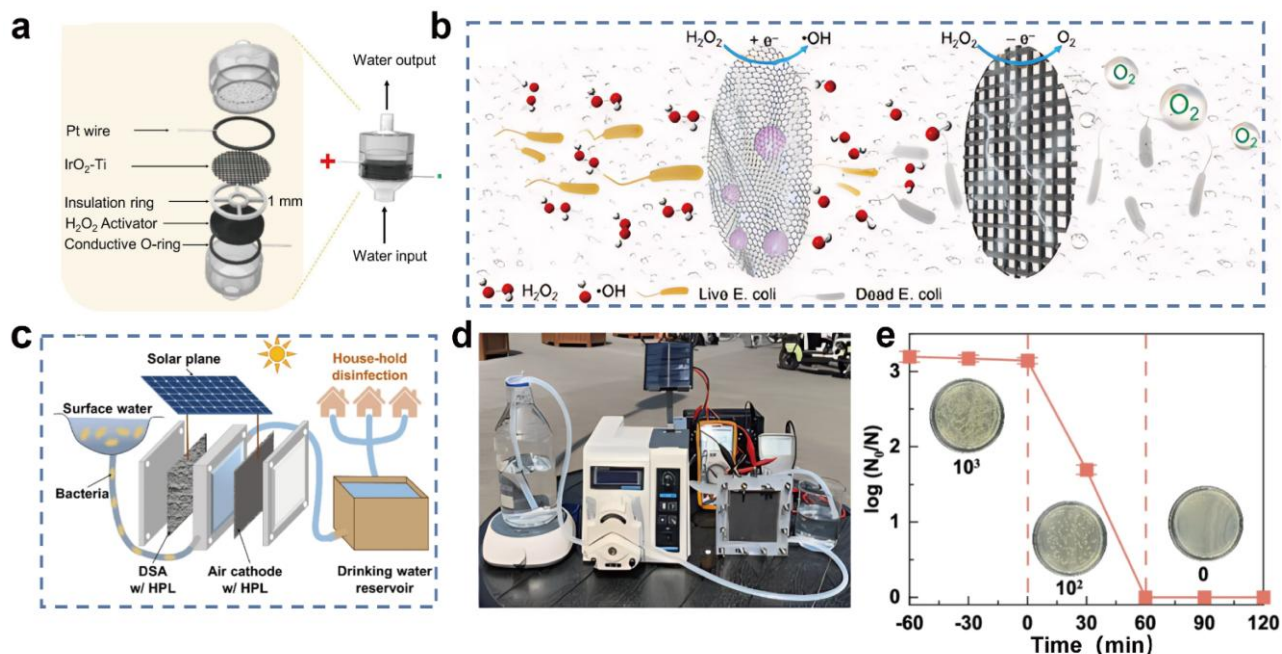


Figure 14. Partial research on H₂O₂ water treatment. (a) Flow-through reactor for tap water disinfection. (b) Schematic drawing of Escherichia coli inactivation.^[109] (Copyright 2023, Elsevier) (c) Schematic illustration and (d) digital image of the solar-driven membrane-free electrolyzer for H₂O₂ electro-synthesis and disinfection. (e) Surface water sterilization of the solar-driven membrane-free electrolyzer.^[110] (Copyright 2025, Springer Nature)

In addition, to boost H₂O₂ production and realize efficient surface water disinfection simultaneously, Yi's group^[110] introduced a polytetrafluoroethylene hydrophobic porous layer (HPL) to improve H₂O₂ generation and combined it with a membrane-free electrolytic cell for surface water disinfection. This configuration achieved complete inactivation of Escherichia coli within 60 minutes (**Figure 14c-e**).

8.3 Degradation of organic substances

To rapidly synthesize high-density fluorine-containing active sites and obtain materials with excellent 2e⁻ ORR performance for the rapid degradation of common dyes, Peng and colleagues^[111] employed plasma ball milling technology to load defect-rich PTFE, with some fluorine atoms removed, onto carbon nanotubes through instantaneous high temperature and ball milling characteristics, thereby achieving the rapid synthesis of high-density fluorine-containing active sites. The developed composite material of defect-rich PTFE with dense fluorine-containing active sites and CNTs exhibited excellent two-electron oxygen reduction performance, enabling the rapid degradation of common dyes such as methylene blue and rhodamine (**Figure 15a-c**). Li's

group^[112] identified molybdenum-doped bismuth tungstate (Bi₂WO₆:Mo) from a series of bismuth-based oxides. This low-cost, highly selective material is ideal for generating H₂O₂ through a two-electron water oxidation reaction. It continuously supplies H₂O₂ for the *in-situ* degradation of persistent pollutants in aqueous solutions. Li et al.^[113] immobilized transition metal manganese (Mn) species onto a porous carbon material (PCM)-based catalyst, yielding the composite catalyst denoted as PCM-DDA-Mn. This PCM-DDA-Mn catalyst not only facilitates the activation of hydrogen peroxide (H₂O₂) but also enhances the generation of hydroxyl radicals (·OH). These synergistic effects ultimately enabled the efficient degradation of humic acid. (**Figure 15d and e**)

8.4 Bleaching

H₂O₂ is a strong oxidizing agent. It can undergo oxidation reactions with pigment molecules, break down the chromophoric groups of the pigments, and make them lose their color. During this reaction, the oxygen element in H₂O₂ changes from the -1 valence to -2 valence or 0 valence, generating water and oxygen, while oxidizing the pigments into colorless substances. It is often used for bleaching fabrics such as cotton,

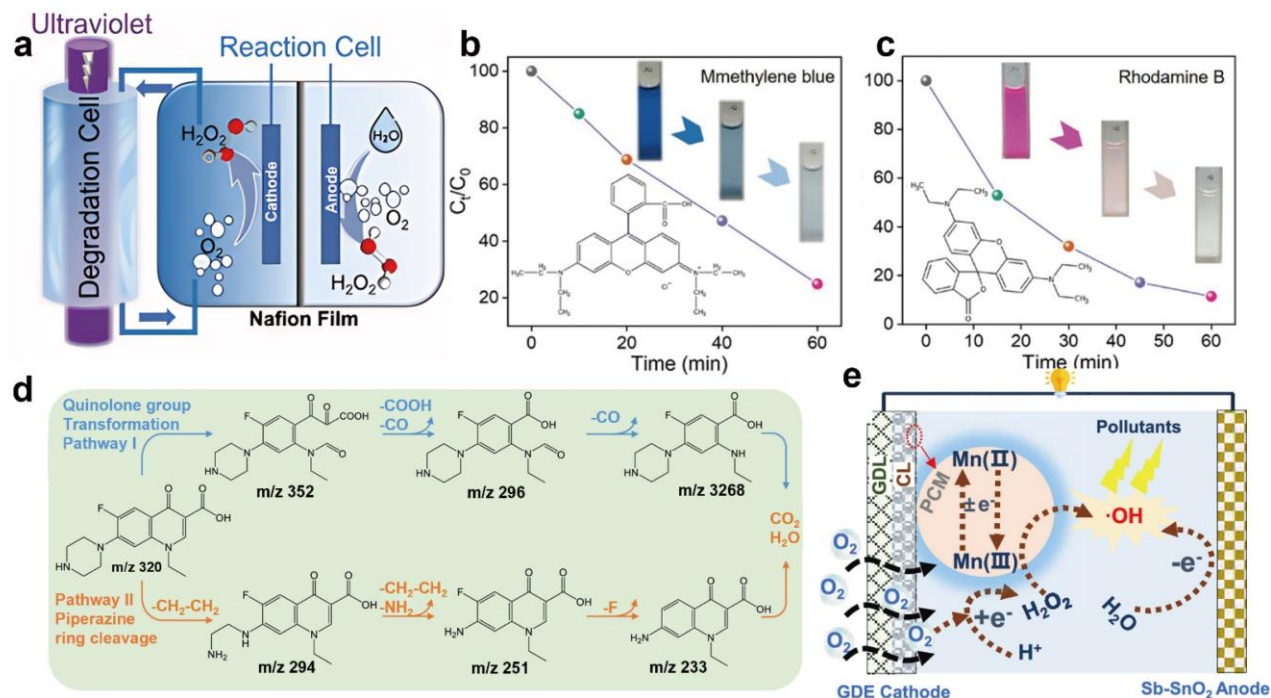


Figure 15. Partial studies on the degradation of organic matter by H₂O₂. (a) The schematic diagram of the dye and antibiotic degradation device. (b) The degradation effect of methylene blue in the device. (c) The degradation effect of Rhodamine B in the device.^[111] (Copyright 2024, Wiley-VCH) (d) Pseudo-first-order rate constant of humic acid removal.^[112] (Copyright 2020, Wiley-VCH) (e) The mechanism diagram of pollutant removal.^[113] (Copyright 2024, American Chemical Society)

linen, and polyester-cotton. It can effectively remove natural pigments and impurities, improve the whiteness of fabrics, and cause less damage to fibers. It is also a crucial reagent for pulp bleaching, which is more ecologically friendly than conventional chlorine bleaching and may eliminate colored materials like lignin while enhancing the whiteness and quality of paper.

8.5 Green oxidizing agents

H₂O₂, as an “environmentally friendly oxidant” can replace toxic/highly polluting oxidants such as potassium permanganate, chromates and fuming sulfuric acid. It is also utilized in the synthesis of numerous chemical raw materials and fine compounds. Nishiguchi and colleagues^[114] effectively developed a green process for producing esomeprazole via an asymmetric sulfoxidation reaction utilizing H₂O₂ as an oxidant in conjunction with iron salts, chiral Schiff bases, and carboxylates.

With continuous breakthroughs in catalyst technology, the application of H₂O₂ in the field of industrial manufacturing will further expand towards the direction of low energy consumption, high efficiency, and high purity, becoming a key supporting

material for the green transformation of industries

9 Challenges and prospects

2e⁻ ORR for H₂O₂ production currently faces three major core challenges. First, balancing the “activity-selectivity-stability” of the catalyst is difficult: precious metal catalysts (Pt, Pd-based) are costly and prone to dissolution/agglomeration; active sites of carbon-based catalysts are unstable under strong acidic/alkaline conditions; metal oxide exhibit low conductivity (10⁻⁴~10⁻² S·cm⁻¹); SACs suffer from low metal loading (typically < 5 wt%) and are prone to migration/agglomeration. Second, large-scale preparation technology is lacking: High-performance catalysts predominantly rely on sophisticated laboratory processes (such as high-temperature calcination for SACs), which involve complex steps, high energy consumption, and are difficult to scale up, and entail high costs. Meanwhile, Kilogram-scale production causes non-uniform heat and mass transfer, leading to inconsistent active-site formation, metal aggregation, and irregular pore structures. Moreover, insufficient mixing and poor temperature control result in low

batch-to-batch reproducibility, while metal leaching and structural instability are aggravated at high loading. Collectively, these issues lead to decreased catalytic activity, lower H_2O_2 selectivity, and poorer stability.^[100,115] Third, the adaptability to practical scenarios is insufficient: the laboratory conditions of “three-electrode + pure electrolyte” are disconnected from reality; there is a lack of an integrated scheme of “catalyst-reactor-renewable energy”; and side reactions are likely to occur in complex media (such as high-salt wastewater).

In response to the above challenges, the following prospects for the innovation of future H_2O_2 preparation technologies are put forward.

(1) Atomic-level precise design of catalysts

It is necessary to precisely regulate the coordination environment of active sites and the electronic structure of catalytic interfaces to break the trade-off among catalytic activity, selectivity, and stability. AI-assisted catalyst design represents an emerging approach to break through the conventional trial-and-error method and accelerate the development of high-performance $2e^-$ ORR catalysts. The core research content includes:^[116] (1) Establishing a catalyst structure – performance database by compiling experimental data (e.g., active site structure, catalytic performance, test conditions) and density functional theory (DFT) calculations (e.g., $^*\text{OOH}$ adsorption energy, reaction energy barrier); (2) Constructing machine learning (ML) models (e.g., random forest, neural network) to correlate catalyst structure with activity/selectivity/stability, thereby enabling predictive screening of high-performance active sites and catalyst compositions; (3) Integrating ML with DFT calculations to optimize reaction conditions (e.g., electrolyte pH, applied potential) and guide the atomic-level precise design of $2e^-$ ORR catalysts (e.g., tuning active site coordination environments, constructing multicomponent synergistic systems).

In addition, by combining DFT, molecular dynamics and continuum models, the model realistically reproduces the actual reaction microenvironment, deconvolutes the contributions of the EDL, solvent, and interface effects, and establishes quantitative relationships between catalyst structure and performance. This enables reliable, operationally relevant predictions for rational catalyst design beyond idealized static calculations.

(2) System integration of catalysts and reactors and adaptation to decentralized application scenarios

To promote decentralized H_2O_2 production, efforts should be made to advance the integration of “catalyst-reactor-renewable energy” systems and design

miniaturized, portable *on-site* preparation devices that couple with photovoltaic or wind power. For specific application scenarios such as water treatment and antibacterial disinfection, optimizing reactor structures and immobilizing catalysts on porous electrodes enable the in-situ generation and immediate utilization of H_2O_2 . Additionally, develop efficient methods for the separation and purification of H_2O_2 , such as using solid-state electrolytes and membrane separation technologies, can reduce downstream processing costs and improve product purity.

(3) Cross-scale mechanism analysis and exploration of emerging catalytic systems

Cross-scale mechanistic investigations spanning atomic-level active site behaviors (e.g., $^*\text{OOH}$ adsorption and desorption) to device-level mass transfer processes (e.g., O_2 diffusion and H^+ transport) are performed to elucidate catalyst deactivation mechanisms and side reaction initiation rules in practical complex electrolytes via in-situ dynamic characterization techniques. While emerging synergistic catalytic systems including photo-electro and enzyme-electro coupling are explored to construct semiconductor-electrocatalyst heterojunctions and bioinspired enzyme-electro hybrid catalysts, further lowering the kinetic barrier of the $2e^-$ ORR to boost the overall efficiency of electrochemical H_2O_2 synthesis.

(1) Techno-economic analysis (TEA)

The industrialization of electrocatalytic H_2O_2 production via the $2e^-$ ORR depends not only on the catalytic performance of catalysts but also on economic feasibility. TEA serves as a key tool for evaluating industrialization potential and optimizing production processes. The core TEA contents for electrocatalytic H_2O_2 production include: (1) calculation of the total production cost; (2) analysis of key cost factors affecting economic feasibility, such as reducing catalyst costs by developing low-cost non-precious metal catalysts and lowering electricity costs by coupling with renewable energy (photovoltaic, wind power); (3) establishment of TEA models for *on-site* H_2O_2 production systems and evaluation of the economic competitiveness of the electrocatalytic route compared with the traditional anthraquinone process. Based on TEA results, targeted optimization strategies (e.g., reactor structure optimization) are proposed to reduce production costs and promote the industrialization of electrocatalytic H_2O_2 production.

CRediT author statement

Jing Zhang and Danni Deng: writing. Fangqiang Wang: visualization. Yu Bai: review. Yuchao Wang: review. Yingbi Chen: review. Peiyao Yang: review. Meng Wang: review. Houzheng Ou:

review. Haitao Zheng: review & editing. Yongpeng Lei: supervision, conceptualization. All authors have given approval to the final version of the manuscript.

Declaration of competing interest

The authors declare that they have no known competing financial interests or personal relationships that could have appeared to influence the work reported in this article. Yongpeng Lei is an Associate Editor of this journal and they were not involved in the editorial review or the decision to publish this article.

Acknowledgments

This work was supported by the National Natural Science Foundation of China (22279165).

References

- [1] Minli Wang, Jinhuan Cheng, Wenwen Xu, Dandan Zhu, Wuyong Zhang, Yingjie Wen, Wanbing Guan, Jinping Jia, Zhiyi Lu. Self-cleaning electrode for stable synthesis of alkaline-earth metal peroxides. *Nature Nanotechnology*, 2025, 20, 67-74. <https://doi.org/10.1038/s41565-024-01815-x>
- [2] Chaoqi Zhang, Pengyue Shan, Yingying Zou, Tong Bao, Xinchang Zhang, Zhijie Li, Yunying Wang, Guangfeng Wei, Chao Liu, Chengzhong Yu. Stable and high-yield hydrogen peroxide electrosynthesis from seawater. *Nature Sustainability*, 2025, 8, 542-552. <https://doi.org/10.1038/s41893-025-01538-4>
- [3] Shilin Yang, Sibe Liu, Hongshan Li, Zhuowen Wang, Jiayu Zhang, Minghui Liu, Jing Ding, Shan Qiu, Fengxia Deng. Boosting oxygen mass transfer for efficient H₂O₂ generation via 2e⁻-ORR: a state-of-the-art overview. *Electrochimica Acta*, 2024, 479, 143889. <https://doi.org/10.1016/j.electacta.2024.143889>
- [4] Chuang Xia, Yang Xia, Peng Zhu, Lei Fan, Haotian Wang. Direct electrosynthesis of pure aqueous H₂O₂ solutions up to 20% by weight using a solid electrolyte. *Science*, 2019, 366, 226-231. <https://doi.org/10.1126/science.aay1844>
- [5] Samuel C. Perry, Dhananjai Pangotra, Lúcia Vieira, Lénárd-István Csepei, Volker Sieber, Ling Wang, Carlos Ponce de León, Frank C. Walsh. Electrochemical synthesis of hydrogen peroxide from water and oxygen. *Nature Reviews Chemistry*, 2019, 3, 442-458. <https://doi.org/10.1038/s41570-019-0110-6>
- [6] Nan Wang, Shaobo Ma, Pengjian Zuo, Jizhou Duan, Baorong Hou. Recent progress of electrochemical production of hydrogen peroxide by two-electron oxygen reduction reaction. *Advanced Science*, 2021, 8, 2100076. <https://doi.org/10.1002/adv.202100076>
- [7] Minghui Zhu, Zhongyue Ge, Zhuying Xu, Xiaofang Liang, Lei Yan, Yulin Sun, Yijun Zhong, Yong Hu. Electrochemical production of H₂O₂ via 2e⁻ ORR and WOR: catalyst design, interface regulation, and scalable device engineering. *Materials Science and Engineering: R: Reports*, 2026, 168, 101168. <https://doi.org/10.1016/j.msere.2025.101168>
- [8] Samira Siahrostami, Arnau Verdaguier-Casadevall, Mohammadreza Karamad, Davide Deiana, Paolo Malacrida, Björn Wickman, María Escudero-Escribano, Elisa A. Paoli, Rasmus Frydendal, Thomas W. Hansen, Ib Chorkendorff, Ifan E. L. Stephens, Jan Rossmeisl. Enabling direct H₂O₂ production through rational electrocatalyst design. *Nature Materials*, 2013, 12, 1137-1143. <https://doi.org/10.1038/nmat3795>
- [9] Danni Deng, Jinxian Wang, Meng Wang, Yuchao Wang, Jiabi Jiang, Yingbi Chen, Yu Bai, Qiumei Wu. Accelerated O₂ adsorption and stabilized *OOH for electrocatalytic H₂O₂ production. *Journal of Materials Science and Technology*, 2025, 227, 76-81. <https://doi.org/10.1016/j.jmst.2024.12.017>
- [10] Yulin Wang, Geoffrey I. N. Waterhouse, Lu Shang, Tierui Zhang. Electrocatalytic oxygen reduction to hydrogen peroxide: from homogeneous to heterogeneous electrocatalysis. *Advanced Energy Materials*, 2021, 11, 2003323. <https://doi.org/10.1002/aenm.202003323>
- [11] Jizhou Jiang, Yanghanbin Zhang, Wei Sun, Jiahe Peng, Weilong Shi, Yang Qu, Enzhou Liu, Arramel, Zhiliang Jin. A review of updated red phosphorus-based photocatalysts. *Composite Functional Materials*, 2025, 1, 20250101. <https://doi.org/10.10521/cfm20250101>
- [12] Yanhui Li, Changhua Wang, Qi Wu, Yuanyuan Li, Shuang Liang, Dexin Jin, He Ma, Xintong Zhang. Bronze TiO₂ photocatalysis facilitates solution plasma production of H₂O₂. *Composite Functional Materials*, 2025, 1, 20250204. <https://doi.org/10.63823/20250204>
- [13] Zhaoyu Wen, Na Han, Yanguang Li. Recent progress towards the production of H₂O₂ by electrochemical two-electron oxygen reduction reaction. *Acta Physico-Chimica Sinica*, 2024, 40, 2304001. <https://doi.org/10.3866/PKU.WHXB.202304001>
- [14] Hongyu Chen, Hao Zhang, Kai Chi, Yan Zhao. Pyrimidine-containing covalent organic frameworks for efficient photosynthesis of hydrogen peroxide via one-step two electron oxygen reduction process. *Nano Research*, 2024, 17, 9498-9506. <https://doi.org/10.1007/s12274-024-6897-6>
- [15] Shanyue He, Xin Zhang, Mei Chen, Hongquan Jiang, Yang Qu, Yanduo Liu, Jizhou Jiang. Photocatalytic H₂O₂ production over Ti(HPO₄)₂ S-scheme heterojunction through push-pull electronic effects enhance the oxygen reduction. *Composite Functional Materials*, 2025, 1, 20250203. <https://doi.org/10.63823/20250203>
- [16] Yuchao Wang, Yi Liu, Wei Liu, Jiao Wu, Qian Li, Qingguo Feng, Zhiyan Chen, Xiang Xiong, Dingsheng Wang, Yongpeng Lei. Regulating the coordination structure of metal single atoms for efficient electrocatalytic CO₂ reduction. *Energy & Environmental Science*, 2020, 13, 4609-4624. <https://doi.org/10.1039/D0EE02833A>

- [17] Xuan Wei, Ying Cao, Yuxing Ma, Rui Cao. Carbon-based electrocatalysts for selective two-electron oxygen reduction. *Catal*, 2026, 2, 5. <https://doi.org/10.1007/s44422-026-00019-9>
- [18] Yanan Shi, Lili Zhang, Chongyang Wang, Shaohui Sun. Heterostructure of Fe₃O₄ confined in hierarchical porous carbon for interface-enhanced medical-grade H₂O₂ electrosynthesis. *Advanced Science*, 2025, 12, 2502388. <https://doi.org/10.1002/advs.202502388>
- [19] Yuanjie Zheng, Peng Wang, Wei-Hsiang Huang, Chiliang Chen, Yanyan Jia, Sheng Dai, Tan Li, Yun Zhao, Yongcai Qiu, Geoffrey I. N. Waterhouse, Guangxu Chen. Toward more efficient carbon-based electrocatalysts for hydrogen peroxide synthesis: roles of cobalt and carbon defects in two-electron ORR catalysis. *Nano Letters*, 2023, 23, 1100-1108. <https://doi.org/10.1021/acs.nanolett.2c0490>
- [20] Helai Huang, Mingze Sun, Shuwei Li, Shengbo Zhang, Yiyang Lee, Zhengwen Li, Jinjie Fang, Chengjin Chen, Yuxiao Zhang, Yanfen Wu, Yizhen Che, Qian Shuairan, Wei Zhu, Cheng Tang, Zhongbin Zhuang, Liang Zhang, Zhiqiang Niu. Enhancing H₂O₂ electrosynthesis at industrial relevant current in acidic media on diatomic cobalt sites. *Journal of the American Chemical Society*, 2024, 146, 9434-9443. <https://doi.org/10.1021/jacs.4c02031>
- [21] Hang Feng, Yinghang Song, Yue Zhang, Qianglong Qi, Chengxu Zhang, Yuebin Feng, Jue Hu. Electronic structure engineering of NiO via cation doping for efficient and stable electrochemical H₂O₂ synthesis. *Chemical Engineering Journal*, 2025, 506, 160364. <https://doi.org/10.1016/j.cej.2025.160364>
- [22] Yuchao Wang, Liang Xu, Longsheng Zhan, Peiyao Yang, Shuaihao Tang, Mengjie Liu, Xin Zhao, Yu Xiong, Zhiyan Chen, Yongpeng Lei. Electron accumulation enables Bi efficient CO₂ reduction for formate production to boost clean Zn-CO₂ batteries. *Nano Energy*, 2022, 92, 106780. <https://doi.org/10.1016/j.nanoen.2021.106780>
- [23] Meng Dan, Ruyi Zhong, Shangyu Hu, Huixiang Wu, Ying Zhou, Zhaoqing Liu. Strategies and challenges on selective electrochemical hydrogen peroxide production: catalyst and reaction medium design. *Chem Catalysis*, 2022, 2, 1919-1960. <https://doi.org/10.1016/j.cheecat.2022.06.002>
- [24] Euiyeon Jung, Heejong Shin, Byoung-Hoo Lee, Vladimir Efremov, Suhyeong Lee, Hyeon Seok Lee, Jiheon Kim, Wytse Hooch Antink, Subin Park, Kug-Seung Lee, Sung-Pyo Cho, Jong Suk Yoo, Yung-Eun Sung, Taeghwan Hyeon. Atomic-level tuning of Co-N-C catalyst for high performance electrochemical H₂O₂ production. *Nature Materials*, 2020, 19, 436-442. <https://doi.org/10.1038/s41563-019-0571-5>
- [25] Minhee Suk, Min Wook Chung, Man Ho Han, Hyung-Suk Oh, Chang Hyuck Choi. Selective H₂O₂ production on surface-oxidized metal-nitrogen-carbon electrocatalysts. *Catalysis Today*, 2021, 359, 99-105. <https://doi.org/10.1016/j.cattod.2019.05.034>
- [26] Danni Deng, Yuchao Wang, Jiabi Jiang, Yu Bai, Yingbi Cheng, Haitao Zheng, Houzheng Ou, Yongpeng Lei. Indium oxide with oxygen vacancies boosts O₂ adsorption and activation for electrocatalytic H₂O₂ production. *Chemical Communications*, 2024, 60, 9364-9367. <https://doi.org/10.1039/D4CC03361B>
- [27] Jie Wu, Yidong Han, Yuchen Bai, Xiting Wang, Yunjie Zhou, Wenxiang Zhu, Tiwei He, Yingming Wang, Hui Huang, Yang Liu, Zhenhui Kang. The electron transport regulation in carbon dots/In₂O₃ electrocatalyst enable 100% selectivity for oxygen reduction to hydrogen peroxide. *Advanced Functional Materials*, 2022, 32, 2203647. <https://doi.org/10.1002/adfm.202203647>
- [28] Edgar Fajardo-Puerto, Abdelhakim Elmouwahidi, Esther Bailon-Garcia, Agustín Francisco Perez-Cadenas, Francisco Carrasco-Marin. From Fenton and ORR 2e⁻-type catalysts to bifunctional electrodes for environmental remediation using the electro-Fenton process. *Catalysts*, 2023, 13, 674. <https://doi.org/10.3390/catal13040674>
- [29] Yang Ou, Yifan Zhang, Wen Luo, Yang Wu, Yong Wang. Rational design of covalent organic frameworks for photocatalytic hydrogen peroxide production. *Macromolecular Rapid Communications*, 2025, 46, 2401149. <https://doi.org/10.1002/marc.202401149>
- [30] Jinwei Xu, Xueli Zheng, Zhiping Feng, Zhiyi Lu, Zewen Zhang, William Huang, Yanbin Li, Djordje Vuckovic, Yuanqing Li, Sheng Dai, Guangxu Chen, Kecheng Wang, Hansen Wang, James K. Chen, William Mitch, Yi Cui. Organic wastewater treatment by a single atom catalyst and electrolytically produced H₂O₂. *Nature Sustainability*, 2021, 4, 233-241. <https://doi.org/10.1038/s41893-020-00635-w>
- [31] Xuan Zhao, Hao Yang, Jie Xu, Tao Cheng, Yanguang Li. Bimetallic PdAu nanoframes for electrochemical H₂O₂ production in acids. *ACS Materials Letters*, 2021, 3, 996-1002. <https://doi.org/10.1021/acsmaterialslett.1c00263>
- [32] Anuj Kumar, Naina Goyal, Sanjay Mathur, Ibragimov Aziz Bakhtiyarovich, Yufeng Zhao, Mohammad Khalid, Mohd Ubaidullah, Abdullah M. Al-Enizi. Advances in coordination engineering of M-N-C single atom catalysts for superior oxygen reduction performance. *Coordination Chemistry Reviews*, 2026, 549, 217244. <https://doi.org/10.1016/j.ccr.2025.217244>
- [33] Jennifer K. Edwards, Adrian Thomas, Albert F. Carley, Andrew A. Herzing, Christopher J. Kiely, Graham J. Hutchings. Au-Pd supported nanocrystals as catalysts for the direct synthesis of hydrogen peroxide from H₂ and O₂. *Green Chemistry*, 2008, 10, 388-394. <https://doi.org/10.1039/B714553P>
- [34] Lyudmila B. Belykh, Nikita I. Skripov, Tatyana P. Sterenchuk, Vladlen V. Akimov, Vladimir L. Tauson, Elena A. Milenkaya, Fedor K. Schmidt. Structurally disordered Pd-P nanoparticles as effective catalysts for the production of hydrogen peroxide by the anthraquinone method. *European Journal of Inorganic Chemistry*, 2021, 2021, 4586-4893.

- <https://doi.org/10.1002/ejic.202100712>
- [35] Yasuhiro Shiraishi, Shunsuke Kanazawa, Yoshitsun Sugano, Daijiro Tsukamoto, Hirokatsu Sakamoto, Satoshi Ichikawa, Takayuki Hirai. Highly selective production of hydrogen peroxide on graphitic carbon nitride (g-C₃N₄) photocatalyst activated by visible light. *ACS Catalysis*, 2014, 4, 774-780. <https://doi.org/10.1021/cs401208c>
- [36] Valentina Perazzolo, Christian Durante, Roberto Pilot, Andrea Paduano, Jian Zheng, Gian Andrea Rizzi, Alessandro Martucci, Gaetano Granozzi, Armando Gennaro. Nitrogen and sulfur doped mesoporous carbon as metal-free electrocatalysts for the in-situ production of hydrogen peroxide. *Carbon*, 2015, 95, 949-963. <https://doi.org/10.1016/j.carbon.2015.09.002>
- [37] Yulin Wang, Run Shi, Lu Shang, Geoffrey I. N. Waterhouse, Jiaqi Zhao, Qinghua Zhang, Lin Gu, Tierui Zhang. High-efficiency oxygen reduction to hydrogen peroxide catalyzed by nickel single-atom catalysts with tetradentate N₂O₂ coordination in a three-phase flow cell. *Angewandte Chemie International Edition*, 2020, 59, 13057-13062. <https://doi.org/10.1002/anie.202004841>
- [38] Shivangi Mehta, Nada Elmerhi, Sukhjot Kaur, Abdul Khayum Mohammed, Tharamani C. Nagaiah, Dinesh Shetty. Modulating core polarity in metal-free covalent organic frameworks for selective electrocatalytic hydrogen peroxide production. *Angewandte Chemie International Edition*, 2025, 64, e202417403. <https://doi.org/10.1002/anie.202417403>
- [39] Ergui Luo, Yuyi Chu, Jie Liu, Zhaoping Shi, Siyuan Zhu, Liyuan Gong, Junjie Ge, Chang Hyuck Choi, Changpeng Liu, Wei Xing. Pyrolyzed M-N_x catalysts for oxygen reduction reaction: progress and prospects. *Energy Environmental Science*, 2021, 14, 2158-2185. <https://doi.org/10.1039/D1EE00142F>
- [40] Samira Siahrostami, Santiago Jimenez Villegas, Amir Hassan Bagherzadeh Mostaghimi, Seoin Back, Amir Barati Farimani, Haotian Wang, Kristin Aslaug Persson, Joseph Montoya. A review on challenges and successes in atomic-scale design of catalysts for electrochemical synthesis of hydrogen peroxide. *ACS Catalysis*, 2020, 10, 7495-7511. <https://doi.org/10.1021/acscatal.0c01641>
- [41] Jiayi Zhang, Haochen Zhang, Mu-Jeng Cheng, Qi Lu. Tailoring the electrochemical production of H₂O₂: strategies for the rational design of high-performance electrocatalysts. *Small*, 2020, 16, 1902845. <https://doi.org/10.1002/sml.201902845>
- [42] Zhiping Deng, Seung Joon Choi, Ge Li, Xiaolei Wang. Advancing H₂O₂ electrosynthesis: enhancing electrochemical systems, unveiling emerging applications, and seizing opportunities. *Chemical Society Reviews*, 2024, 53, 8137-8181. <https://doi.org/10.1039/D4CS00412D>
- [43] Yiran Sun, Changqu Liu, Shuqi Ji, Jinbo Ni, Xiangning Wu, Sembukuttiarachilage Ravi Pradip Silva, Meng Cai, Guosheng Shao, Peng Zhang. Hollow-structured materials for advanced energy storage and conversion: rational synthesis, multifunctional applications, and mechanism insights. *Composite Functional Materials*, 2025, 1, 20250202. <https://doi.org/10.63823/20250202>
- [44] Shanyong Chen, Tao Luo, Xiaoqing Li, Kejun Chen, Junwei Fu, Kang Liu, Chao Cai, Qiyong Wang, Hongmei Li, Yu Chen, Chao Ma, Li Zhu, Ying-Rui Lu, Ting-Shan Chan, Mingshan Zhu, Emiliano Cortés, Min Liu. Identification of the highly active Co-N₄ coordination motif for selective oxygen reduction to hydrogen peroxide. *Journal of the American Chemical Society*, 2022, 144, 14505-14516. <https://doi.org/10.1021/jacs.2c01194>
- [45] Ambarish Kulkarni, Samira Siahrostami, Anjali Patel, Jens K. Nørskov. Understanding catalytic activity trends in the oxygen reduction reaction. *Chemical Reviews*, 2018, 118, 2302-2312. <https://doi.org/10.1021/acs.chemrev.7b00488>
- [46] Zhiyong Yu, Shengyao Lv, Qing Yao, Nan Fang, Yong Xu, Qi Shao, Chih-Wen Pao, Jyh-Fu Lee, Guoliang Li, Li-Ming Yang, Xiaoqing Huang. Low-coordinated Pd site within amorphous palladium selenide for active, selective, and stable H₂O₂ electrosynthesis. *Advanced Materials*, 2023, 35, 2208101. <https://doi.org/10.1002/adma.202208101>
- [47] Zuozhong Liang, Haitao Lei, Haoquan Zheng, Hong-Yan Wang, Wei Zhang, Rui Cao. Selective two-electron and four-electron oxygen reduction reactions using Co-based electrocatalysts. *Chemical Society Reviews*, 2025, 54, 5248-5291. <https://doi.org/10.1039/D4CS01199F>
- [48] Kun Jiang, Jiajun Zhao, Haotian Wang. Catalyst design for electrochemical oxygen reduction toward hydrogen peroxide. *Advanced Functional Materials*, 2020, 30, 2003321. <https://doi.org/10.1002/adfm.202003321>
- [49] Zhuoqi Zhou, Yu Han, Manman Zou, Ronglan Pan, Xin Ge, Chuanxun Du, Jili Yuan, Tao Wang, Hao Zhang, Hu Li, Jian Zhang. Boosting hydrogen spillover over carbon nanotube anchored ultrafine Co/Co₂O₃ nanoparticles for efficient neutral H₂O₂ electrosynthesis. *Rare Metals*, 2025, 44, 8619-8631. <https://doi.org/10.1007/s12598-025-03557-8>
- [50] Erzhuo Zhao, Wendan Xue, Shuhan Qin, Yang Guo, Xin Xin, Huijiao Wang, Yinqiao Zhang, Sijin Zuo. A review of H₂O₂ electrosynthesis by 2-electron ORR and 2-electron WOR: from catalysts to electrochemical cells. *Coordination Chemistry Reviews*, 2026, 545, 217042. <https://doi.org/10.1016/j.ccr.2025.217042>
- [51] Rong Ma, Gao-Feng Han, Feng Li, Yunfei Bu. Rational design of carbon-based electrocatalysts for H₂O₂ production by machine learning and structural engineering. *Advanced Energy Materials*, 2025, 15, 2500953. <https://doi.org/10.1002/aenm.202500953>
- [52] Tiantian Lu, Mingzi Sun, Fengmei Wang, Shan Chen, Youzeng Li, Jialei Chen, Xuelong Liao, Xiaoting Sun, Ying Liu, Fei Wang, Bolong Huang, Huan Wang. Selective oxidation of sp-bonded carbon in graphdiyne/carbon nanotubes heterostructures to form dominant epoxy groups for

- two-electron oxygen reduction. *ACS Nano*, 2024, 18, 15035-15045. <https://doi.org/10.1021/acsnano.4c01698>
- [53] Jiangbo Xi, Sungeun Yang, Luca Silvioli, Sufeng Cao, Pei Liu, Qiongyang Chen, Yanyan Zhao, Hongyu Sun, Johannes Novak Hansen, Jens-Peter B. Haraldste, Jakob Kibsgaard, Jan Rossmeisl, Sara Bals, Shuai Wang, Ib Chorkendorff. Highly active, selective, and stable Pd single-atom catalyst anchored on N-doped hollow carbon sphere for electrochemical H₂O₂ synthesis under acidic conditions. *Journal of Catalysis*, 2021, 393, 313-323. <https://doi.org/10.1016/j.jcat.2020.11.020>
- [54] Shan Ding, Baokai Xia, Ming Li, Fengqian Lou, Chi Cheng, Tianqi Gao, Yuxiang Zhang, Kang Yang, Lili Jiang, Zhihao Nie, Hongxin Guan, Jingjing Duan, Sheng Chen. An abnormal size effect enables ampere-level O₂ electroreduction to hydrogen peroxide in neutral electrolytes. *Energy Environmental Science*, 2023, 16, 3363-3372. <https://doi.org/10.1039/D3EE00509G>
- [55] Sungeun Yang, Arnau Verdager-Casadevall, Logi Arnarson, Luca Silvioli, Viktor Čolić, Rasmus Frydendal, Jan Rossmeisl, Ib Chorkendorff, Ifan E L Stephens. Toward the decentralized electrochemical production of H₂O₂: a focus on the catalysis. *ACS Catalysis*, 2018, 8, 4064-4081. <https://doi.org/10.1021/ACSCATAL.8B00217>
- [56] Jinqi Li, Yuewei Deng, Yingzhang Shi, Jiayi Guo, Shuang Li, Chen Huang, Wenda Zhang, Zhiwen Wang, Yujie Song, Ling Wu. Regulating 2e⁻ ORR on Ag clusters modified CdS nanosheets for enhancing photocatalytic HMF directional oxidation coupled with H₂O₂ evolution. *Chemical Engineering Journal*, 2025, 520, 166375. <https://doi.org/10.1016/j.cej.2025.166375>
- [57] Genwang Zhu, Shuaijie Zhao, Yueling Yu, Xinfei Fan, Kaiyuan Liu, Xie Quan, Yanming Liu. Tuning local proton concentration and *OOH intermediate generation for efficient acidic H₂O₂ electrosynthesis at ampere-level current density. *Angewandte Chemie International Edition*, 2025, 64, e202503626. <https://doi.org/10.1002/anie.202503626>
- [58] Jiabi Jiang, Yuchao Wang, Danni Deng, Yingbi Chen, Yu Bai, Meng Wang, Xiang Xiong, Yongpeng Lei. Hydroxyl combined with nitrogen on biomass carbon promotes the electrocatalytic H₂O₂ selectivity. *Journal of Metals, Materials and Minerals*, 2025, 35, e2216. <https://doi.org/10.55713/jmmm.v35i1.2216>
- [59] Danni Deng, Jiao Wu, Qingguo Feng, Xin Zhao, Mengjie Liu, Yu Bai, Jinxian Wang, Xinran Zheng, Jiabi Jiang, Zechao Zhuang, Xiang Xiong, Dingsheng Wang, Yongpeng Lei. Highly reversible zinc-air batteries at -40 °C enabled by anion-mediated biomimetic. *Advanced Functional Materials*, 2024, 34, 2308762. <https://doi.org/10.1002/adfm.202308762>
- [60] Penghuan Liu, Yicong Li, Changchun Sun, Guiju Liu, Xiaohan Wang, Haiguang Zhao. Atomic-level Co/mesoporous carbon nanofibers for efficient electrochemical H₂O₂ production. *ACS Applied Nano Materials*, 2025, 8, 7267-7277. <https://doi.org/10.1021/acsnm.5c00621>
- [61] Kaiming Li, Ben Huang, Aihao Xu, Kai Nie, Xianhai Bai, Qian Ning, Guodong Wang, Shiming Qiu, Huibing He, Yang Ren, Jing Xu, Xucai Yin. Regulating interfacial hydrogen-bonding connectivity by oxygen vacancies-driven [Fe(CN)₆]³⁻ coordination for boosting hydrogen peroxide electrosynthesis. *Carbon Energy*, 2026, 8, e70147. <https://doi.org/10.1002/cey2.70147>
- [62] Yanping Zhu, Chenlu Yang, Tongchan Lu, Yizhen Gan, Hao Zhao, Yubin Chen, Qingqing Cheng, Hui Yang. Engineering spin state of CoN₄-C single atom catalyst for acidic electrosynthesis of hydrogen peroxide. *Nano Energy*, 2025, 141, 111142. <https://doi.org/10.1016/j.nanoen.2025.111142>
- [63] Xin Zhao, Qingguo Feng, Mengjie Liu, Yuchao Wang, Wei Liu, Danni Deng, Jiabi Jiang, Xinran Zheng, Longsheng Zhan, Jinxian Wang, Huanran Zheng, Yu Bai, Yingbi Chen, Xiang Xiong, Yongpeng Lei. Built-in electric field promotes interfacial adsorption and activation of CO₂ for C₁ products over a wide potential window. *ACS Nano*, 2024, 18, 9678-9687. <https://doi.org/10.1021/acsnano.4c01190>
- [64] Yu Bai, Danni Deng, Jinxian Wang, Yuchao Wang, Yingbi Chen, Huanran Zheng, Mengjie Liu, Xinran Zheng, Jiabi Jiang, Haitao Zheng, Maozhong Yi, Weijie Li, Guozhao Fang, Dingsheng Wang, Yongpeng Lei. Inhibited passivation by bioinspired cell membrane Zn interface for Zn-air batteries with extended temperature adaptability. *Advanced Materials*, 2024, 36, 2411404. <https://doi.org/10.1002/adma.202411404>
- [65] Yuanjie Zheng, Peng Wang, Wei-Hsiang Huang, Chi-Liang Chen, Yanyan Jia, Sheng Dai, Tan Li, Yun Zhao, Yongcai Qiu, Geoffrey I.N. Waterhouse, Guangxu Chen. Toward more efficient carbon-based electrocatalysts for hydrogen peroxide synthesis: roles of cobalt and carbon defects in two-electron ORR catalysis. *Nano Letters*, 2023, 23, 1100-1108. <https://doi.org/10.1021/acs.nanolett.2c04901>
- [66] Yuhan Wu, Yuying Zhao, Qixin Yuan, Hao Sun, Ao Wang, Kang Sun, Geoffrey I. N. Waterhouse, Ziyun Wang, Jingjie Wu, Jianchun Jiang, Mengmeng Fan. Electrochemically synthesized H₂O₂ at industrial-level current densities enabled by in situ fabricated few-layer boron nanosheets. *Nature Communications*, 2024, 15, 10843. <https://doi.org/10.1038/s41467-024-55071-7>
- [67] Yingbi Chen, Qingguo Feng, Yu Bai, Meng Wang, Yuchao Wang, Peiyao Yang, Danni Deng, Xinran Zheng, Jiabi Jiang, Haitao Zheng, Guozhao Fang, Yi Zeng, Xiang Xiong, Yongpeng Lei. Phosphorus-induced electron pump enhances O₂ activation for electrocatalytic H₂O₂ production. *ACS Nano*, 2025, 19, 28801-28812. <https://doi.org/10.1021/acsnano.5c08610>
- [68] Shinuo Liang, Fengjun Li, Fei Huang, Xinyu Wang, Shengwei Liu. Modulating electronic structure of g-C₃N₄ hosted Co-N₄ active sites by axial phosphorus coordination for efficient overall H₂O₂ photosynthesis from oxygen and water. *Chinese Journal of Catalysis*. 2025, 76, 81-95. [https://doi.org/10.1016/S1872-2067\(25\)64735-8](https://doi.org/10.1016/S1872-2067(25)64735-8)

- [69] Ronggen Zhang, Tong Wu, Zongye Yue, Junping Zhang, Shenghua Chen, Pei Feng. Engineering the electronic structure of atomically dispersed p-block bismuth sites via multi-shells tuning effect for boosting oxygen reduction reaction. *Nano Research*, 2025, 18, 94907591. <https://doi.org/10.26599/NR.2025.94907591>
- [70] Yu Gu, Yingjun Tan, Hao Tan, Ying Han, Dongfang Cheng, Fangxu Lin, Zhengyi Qian, Lingyou Zeng, Shipeng Zhang, Ruijin Zeng, Youxing Liu, Hongyu Guo, Mingchuan Luo, Shaojun Guo. Industrial electrosynthesis of hydrogen peroxide over p-block metal single sites. *Nature Synthesis*, 2025, 4, 614-621. <https://doi.org/10.1038/s44160-024-00722-2>
- [71] Tiantian Lu, Ying Liu, Youzeng Li, Jialei Chen, Shan Chen, Xuelong Liao, Wei Xia, Tong Zhou, Wei Wang, Zhou Chen, Rong Huang, Huan Wang. Identifying catalytic sites in oxygen-modified cobalt single atoms for H₂O₂ electrosynthesis and in situ realizing electro-Fenton process in acid. *Applied Catalysis B: Environment and Energy*, 2025, 365, 124949. <https://doi.org/10.1016/j.apcatb.2024.124949>
- [72] Zewen Zhuang, Aijian Huang, Xin Tan, Kaian Sun, Chen Chen, Qing Peng, Zhongbin Zhuang, Tong Han, Hai Xiao, Yuan Zeng, Wei Yan, Jiujun Zhang, Yadong Li. P-block-metal bismuth-based electrocatalysts featuring tunable selectivity for high-performance oxygen reduction reaction. *Joule*, 2023, 7, 1003-1015. <https://doi.org/10.1016/j.joule.2023.04.005>
- [73] Hongjing He, Shuling Liu, Yanyan Liu, Limin Zhou, Hao Wen, Ruofan Shen, Huanhuan Zhang, Xianji Guo, Jianchun Jiang, Baojun Li. Review and perspectives on carbon-based electrocatalysts for the production of H₂O₂ via two-electron oxygen reduction. *Green Chemistry*, 2023, 25, 9501-9542. <https://doi.org/10.1039/D3GC02856A>
- [74] Jingjing Jia, Zhenxin Li, Yunrui Tian, Xia Li, Rui Chen, Jiachen Liu, Ji Liang. Electrosynthesis of H₂O₂ via two-electron oxygen reduction over carbon-based catalysts: From microenvironment control to electrode/reactor design. *Energy Reviews*, 2024, 3, 100069. <https://doi.org/10.1016/j.enrev.2024.100069>
- [75] Caroline de O. Carrilho, Juliana M.S. de Jesus, João Paulo C. Moura, Dara Silva Santos, Aline B. Trench, Caio Machado Fernandes, Aila O. Santos, Odivaldo C. Alves, Júlio C.M. Silva, Mauro C. dos Santos. Influence of CeO₂MnOx heterostructure on hydrogen peroxide electrogeneration on carbon-based catalysts. *Electrochimica Acta*, 2026, 550, 148125. <https://doi.org/10.1016/j.electacta.2026.148125>
- [76] Wei Peng, Jiabin Liu, Xiaoqing Liu, Liqun Wang, Lichang Yin, Haotian Tan, Feng Hou, Ji Liang. Facilitating two-electron oxygen reduction with pyrrolic nitrogen sites for electrochemical hydrogen peroxide production. *Nature Communications*, 2023, 14, 4430. <https://doi.org/10.1038/s41467-023-40118-y>
- [77] Fei Xiang, Xuhong Zhao, Jian Yang, Ning Li, Wenxiao Gong, Yizhen Liu, Arturo Burguete-Lopez, Yulan Li, Xiaobin Niu, Andrea Fratolocchi. Enhanced selectivity in the electroproduction of H₂O₂ via F/S dual-doping in metal-free nanofibers. *Advanced Materials*, 2023, 35, 2208533. <https://doi.org/10.1002/adma.202208533>
- [78] Jae Won Choi, Ayeong Byeon, Sooyeon Kim, Chang-Kyu Hwang, Wenjun Zhang, Jimin Lee, Won Chan Yun, Sae Yane Paek, Jin Hyeung Kim, Giho Jeong, Seung Yong Lee, Joonhee Moon, Sang Soo Han, Jae W. Lee, Jong Min Kim. Mesoporous boron-doped carbon with curved B₄C active sites for highly efficient H₂O₂ electrosynthesis in neutral media and air supplied environments. *Advanced Materials*, 2025, 37, 2415712. <https://doi.org/10.1002/adma.202415712>
- [79] Zhixiong Song, Xiao Chi, Shu Dong, Biao Meng, Xiaojiang Yu, Xiaoling Liu, Yu Zhou, Jun Wang. Carboxylated hexagonal boron nitride/graphene configuration for electrosynthesis of high-concentration neutral hydrogen peroxide. *Angewandte Chemie International Edition*, 2024, 63, e202317267. <https://doi.org/10.1002/anie.202317267>
- [80] Kewang Liu, Fei Li, Haiyin Zhan, Sihui Zhan. Recent progress in two-dimensional materials for generation of hydrogen peroxide by two-electron oxygen reduction reaction. *Materials Today Energy*, 2024, 40, 101500. <https://doi.org/10.1016/j.mtener.2024.101500>
- [81] Monica Rigoletto, Enzo Laurenti, Maria Laura Tummino. An overview of environmental catalysis mediated by hydrogen peroxide. *Catalysts*, 2024, 14, 267. <https://doi.org/10.3390/catal14040267>
- [82] Hongyuan Sheng, Aurora N. Janes, R. Dominic Ross, Dave Kaiman, Jinzhen Huang, Bo Song, J. R. Schmidt, Song Jin. Stable and selective electrosynthesis of hydrogen peroxide and the electro-Fenton process on CoSe₂ polymorph catalysts. *Energy Environmental Science*, 2020, 13, 4189-4203. <https://doi.org/10.1039/D0EE01925A>
- [83] Xiaowei Cai, Fei Peng, Xingyu Luo, Xuejie Ye, Junxi Zhou, Xiaoling Lang, Meiqin Shi. Understanding the evolution of cobalt-based metal-organic frameworks in electrocatalysis for the oxygen evolution reaction. *ChemSusChem*, 2021, 14, 3163-3173. <https://doi.org/10.1002/cssc.202100851>
- [84] Meihuan Liu, Hui Su, Weiren Cheng, Feifan Yu, Yuanli Li, Wanlin Zhou, Hui Zhang, Xuan Sun, Xiuxiu Zhang, Shiqiang Wei, Qinghua Liu. Synergetic dual-ion centers boosting metal organic framework alloy catalysts toward efficient two electron oxygen reduction. *Small*, 2022, 18, 2202248. <https://doi.org/10.1002/sml.202202248>
- [85] Chaoqi Zhang, Ling Yuan, Chao Liu, Zimeng Li, Yingying Zou, Xinchang Zhang, Yue Zhang, Zhiqiang Zhang, Guangfeng Wei, Chengzhong Yu. Crystal engineering enables cobalt-based metalorganic frameworks as high-performance electrocatalysts for H₂O₂ production. *Journal of the American Chemical Society*, 2023, 145, 7791-7799. <https://doi.org/10.1021/jacs.2c11446>
- [86] Yunjie Zhou, Liang Xu, Jie Wu, Wenxiang Zhu, Tiwei He, Hao Yang, Hui Hung, Tao Cheng, Yang Liu, Zhenhui Kang.

- The operation active site of O₂ reduction to H₂O₂ over ZnO. *Energy Environmental Science*, 2023, 16, 3526-3533. <https://doi.org/10.1039/D3EE01788E>
- [87] Zekun Wu, Tianzuo Wang Ji-Jun Zou, Yongdan Li, Cuijuan Zhang. Amorphous nickel oxides supported on carbon nanosheets as high-performance catalysts for electrochemical synthesis of hydrogen peroxide. *ACS Catalysis*, 2022, 12, 5911-5920. <https://doi.org/10.1021/acscatal.2c01829>
- [88] Yue Huang, Jinfeng Zhang, Olim Ruzimuradov, Shavkat Mamatkulov, Kai Dai, Jingxiang Low. Selective oxygen vacancy engineering for shrinking the potential barrier of S-scheme heterojunction toward highly efficient photocatalytic CO₂ conversion. *Composite Functional Materials*, 2025, 1, 20250103. <https://doi.org/10.63823/20250103>
- [89] Yuchao Wang, Qian Li, Meng Wang, Houzheng Ou, Danni Deng, Huanran Zheng, Yu Bai, Lirong Zheng, Zhi-Yan Chen, Weijie Li, Guozhao Fang, Yongpeng Lei. Pumping electrons from oxygen-bridged cobalt for low-charging voltage Zn-air batteries. *Nano Letters*, 2024, 24, 13653-13661. <https://doi.org/10.1021/acs.nanolett.4c03510>
- [90] Huanran Zheng, Danni Deng, Xinran Zheng, Yingbi Chen, Yu Bai, Mengjie Liu, Jiabi Jiang, Haitao Zheng, Yuchao Wang, Jinxian Wang, Peiyao Yang, Yu Xiong, Xiang Xiong, Yongpeng Lei. Highly reversible Zn-air batteries enabled by tuned valence electron and steric hindrance on atomic Fe-N₄-C sites. *Nano Letters*, 2024, 24, 4672-4681. <https://doi.org/10.1021/acs.nanolett.4c01078>
- [91] Ying-Xia Du, Qiao Yang, Wang-Ting Lu, Qing-Yu Guan, Fei-Fei Cao, Geng Zhang. Carbon black-supported single-atom Co-N-C as an efficient oxygen reduction electrocatalyst for H₂O₂ production in acidic media and microbial fuel cell in neutral media. *Advanced Functional Materials*, 2023, 33, 2300895. <https://doi.org/10.1002/adfm.202300895>
- [92] Rui Chen, Wei Liua, Zhiyuan Sang, Jingjing Jia, Zhenxin Li, Jiahuan Nie, Qiao Jiang, Zixian Mao, Baitong Guo, Qiuying Wang, Feng Hou, Lichang Yin, De'an Yang, Ji Liang. Identification of the highly active Zn-N₄ sites with pyrrole/pyridine-N synergistic coordination by dz²⁺s-band center for electrocatalytic H₂O₂ production. *Journal of Energy Chemistry*, 2024, 98, 105-113. <https://doi.org/10.1016/j.jechem.2024.06.021>
- [93] Longxiang Liu, Liqun Kang, Jianrui Feng, David G. Hopkinson, Christopher S. Allen, Yeshu Tan, Hao Gu, Iuliia Mikulska, Veronica Celorrio, Diego Gianolio, Tianlei Wang, Liquan Zhang, Kaiqi Li, Jichao Zhang, Jiexin Zhu, Georg Held, Pilar Ferrer, David Grinter, June Callison, Martin Wilding, Sining Chen, Ivan Parkin, Guanjie He. Atomically dispersed asymmetric cobalt electrocatalyst for efficient hydrogen peroxide production in neutral media. *Nature Communications*, 2024, 15, 4079. <https://doi.org/10.1038/s41467-024-48209-0>
- [94] Shanyong Chen, Tao Luo, Jingyu Wang, Jiaqi Xiang, Xiaoqing Li, Chao Ma, Cheng-wei Kao, Ting-Shan Chan, You-Nian Liu, Min Liu. Tuning proton affinity on Co-N-C atomic interface to disentangle activity-selectivity trade-off in acidic oxygen reduction to H₂O₂. *Angewandte Chemie International Edition*, 2025, 137, e202418713. <https://doi.org/10.1002/anie.202418713>
- [95] Yuan Zeng, Xin Tan, Zewen Zhuang, Chen Chen, Qing Peng. Nature-inspired N, O Co-coordinated manganese single-atom catalyst for efficient hydrogen peroxide electrosynthesis. *Angewandte Chemie International Edition*, 2025, 64: e202416715. <https://doi.org/10.1002/anie.202416715>
- [96] Ruipeng Yuan, Jinyu Zhao, Xu Chen, Xiaoming Qiu, Xiaomin Wang. Inhibiting carbon corrosion of cobalt-nitrogen-carbon materials via Mn sites for highly durable oxygen reduction reaction in acidic media. *Journal of Colloid and Interface Science*, 2025, 680, 712-722. <https://doi.org/10.1016/j.jcis.2024.11.115>
- [97] Xiaomei Liu, Jingkun An, Nan Li, Qicheng Zhang, Yang Li, Jiapeng Liu, Xiaoguang Duan, Xiaobin Fan, Yung-Kang Peng, Wencho Peng. Pentagonal defects enriched carbon fibers for enhanced H₂O₂ electrosynthesis. *Applied Catalysis B: Environment and Energy*, 2026, 386, 126379. <https://doi.org/10.1016/j.apcatb.2025.126379>
- [98] Jiabin Su, Lei Jiang, Bingbing Xiao, Zixian Liu, Heng Wang, Yongfa Zhu, Jun Wang, Xiaofeng Zhu. Dipole-dipole tuned electronic reconfiguration of defective carbon sites for efficient oxygen reduction into H₂O₂. *Small*, 2024, 20, 2310317. <https://doi.org/10.1002/sml.202310317>
- [99] Liangjie Fu, Zixiong Li, Yimin Wu, Aidong Tang, Huaming Yang. Adjusted MnO oxygen vacancy for highly selective ORR production of H₂O₂. *Chemical Communications*, 2024, 60, 8091-8094. <https://doi.org/10.1039/D4CC01614A>
- [100] Yongfei Cui, Wenzheng Zhou, Huarui Yang, Danning Li, Hongyan Han, Yuhang Zhang, Steve Dunn. Lattice distortion and morphology modulation enhanced piezocatalytic activity of Ca-doped Sr₂Nb₂O₇ towards H₂O₂ production and piezo-self-Fenton degradation. *Nano Energy*, 2025, 146, 111540. <https://doi.org/10.1016/j.nanoen.2025.111540>
- [101] Xinyi Zhang, Xiaoxuan Yang, Boman Su, Yu Gu, Bin Yang, Zhongjian Li, Qinghua Zhang, Lecheng Lei, Liming Dai, Yang Hou. Membrane electrode assembly for hydrogen peroxide electrosynthesis. *Nature Reviews Clean Technology*, 2025, 1, 413-431. <https://doi.org/10.1038/s44359-025-00069-7>
- [102] Yihe Chen, Cheng Zhen, Yubin Chen, Hao Zhao, Yuda Wang, Zhouying Yue, Qiansen Wang, Jun Li, M. Danny Gu, Qingqing Cheng, Hui Yang. Oxygen functional groups regulate cobalt-porphyrin molecular electrocatalyst for acidic H₂O₂ electrosynthesis at industrial-level current. *Angewandte Chemie International Edition*, 2024, 63, e202407163. <https://doi.org/10.1002/anie.202407163>
- [103] Jiahuan Nie, Zhenxin Li, Wei Liu, Zhiyuan Sang, De'an Yang, Liqun Wang, Feng Hou, Ji Liang. Recent progress in oxygen reduction reaction toward hydrogen peroxide electrosynthesis and cooperative coupling of anodic reactions. *Advanced*

- Materials, 2025, 37, e2420236. <https://doi.org/10.1002/adma.202420236>
- [104] Erzhao Zhao, Yixin Zhang, Juhong Zhan, Guangsen Xia, Gang Yu, Yujue Wang. Optimization and scaling-up of porous solid electrolyte electrochemical reactors for hydrogen peroxide electrosynthesis. *Nature Communications*, 2025, 16, 3212. <https://doi.org/10.1038/s41467-025-58385-2>
- [105] Ye Tian, Luwei Pei, Shuo Wang, Kongrui Yu, Yuqing Xu, Xiaoqin Ye, Songming Zhu, Ying Liu, Zhenghua Zhang, Zhangying Ye. A self-breathing electrode enabled by interface regulation and gradient wettability engineering for industrial H₂O₂ electrosynthesis. *Nature Communications*, 2026, 17, 1735. <https://www.nature.com/articles/s41467-026-68436-x>
- [106] Meng Zhang, Jia-Run Huang, Cheng-Peng Liang, Xiao-Ming Chen, Pei-Qin Liao. Continuous electrosynthesis of pure H₂O₂ solution with medical-grade concentration by a conductive Ni-phthalocyanine based covalent organic framework. *Journal of the American Chemical Society*, 2024, 146, 31034-31041. <https://doi.org/10.1021/jacs.4c10675>
- [107] Ying Huang, Zi Fu, Han Wang, Zeyang Liu, Mengqi Gao, Yanran Luo, Meng Zhang, Jing Wang, Dalong Ni. Calcium peroxide-based hydrogels enable biphasic release of hydrogen peroxide for infected wound healing. *Advanced Science*, 2024, 11, 2404813. <https://doi.org/10.1002/adv.202404813>
- [108] Chenxi Wu, Yu Gao, Guixi Hu, Bangcheng Yang, Siqi Zhang, Yuting Chen, Jing Chen, Yong Liu, Congling Kong. Zn⁰@ZIF-8 activated O₂ for H₂O₂ generation: synergistic bacteria deactivation and wound healing. *Journal of Colloid and Interface Science*, 2026, 701, 138716. <https://doi.org/10.1016/j.jcis.2025.138716>
- [109] Xue Wen, Xiangcheng Zhang, Meng Wang, Congli Yuan, Junyu Lang, Xue Li, Hao Wei, Daniel Mandler, Mingce Long. Efficient electrocatalytic H₂O₂ activation over nitrogen-doped carbon encapsulated Co₃O₄ for drinking water disinfection. *Applied Catalysis B: Environmental*, 2024, 342, 123437. <https://doi.org/10.1016/j.apcatb.2023.123437>
- [110] Kexin Yi, Chao Li, Shaogang Hu, Xiayu Yuan, Bruce E. Logan, Wulin Yang. High H₂O₂ production in membrane-free electrolyzer via anodic bubble shielding towards robust rural disinfection. *Nature Communications*, 2025, 16, 1893. <https://doi.org/10.1038/s41467-025-57116-x>
- [111] Wei Peng, Jiacheng Qiu, Xiaoqing Liu, Haotian Tan, Feng Hou, Jianmin Feng, Xiao Yan, Ji Liang. Defective PTFE with dense active sites enabling rapid H₂O₂ production for efficient water purification. *Advanced Functional Materials*, 2024, 34, 2411353. <https://doi.org/10.1002/adfm.202411353>
- [112] Lejing Li, Zhuofeng Hu, Jimmy C. Yu. On-demand synthesis of H₂O₂ by water oxidation for sustainable resource production and organic pollutant degradation. *Angewandte Chemie International Edition*, 2020, 59, 20538. <https://doi.org/10.1002/anie.202008031>
- [113] Xuechuan Li, Sen Lu, Nan Chen, Siyuan Chen, Hyoungh-il Kim, Guan Zhang. Molecular-level tuning of active sites of the carbonaceous catalyst for boosting electrochemical H₂O₂ production and its application in electro-Fenton-like degradation of organics. *ACS ES&T Engineering*, 2024, 4, 1690-1701. <https://doi.org/10.1021/acsestengg.4c00084>
- [114] Chaoqi Zhang, Pengyue Shan, Yingying Zou, Tong Bao, Xinchun Zhang, Zhijie Li, Yunying Wang, Guangfeng Wei, Chao Liu, Chengzhong Yu. Stable and high-yield hydrogen peroxide electrosynthesis from seawater. *Nature Sustainability*, 2025, 8, 542-552. <https://doi.org/10.1038/s41893-025-01538-4>
- [115] Ipsita Mondal, Hongyuan Sheng, Kwanpyung Lee, Song Jin, J. R. Schmidt. Rationalizing the overall H₂O₂ selectivity of metal dichalcogenide electrocatalysts for the two-electron oxygen reduction reaction using microkinetic modeling. *ACS Catalysis*, 2025, 15, 8788-8798. <https://doi.org/10.1021/acscatal.5c01079>
- [116] Shigenobu Nishiguchi, Takuhiro Izumi, Tatsuya Yamada, Takayoshi Kouno, Laurean Ilies. Development of a safe and environmentally benign manufacturing process for esomeprazole using an iron catalyst and hydrogen peroxide. *Organic Process Research & Development*, 2024, 28, 3396-3403. <https://doi.org/10.1021/acs.oprd.4c00250>